

Use of Acoustic Emission to Study Deformation of Mild Steel
in Hydrogen and Nitrogen Environments

by

John C. Fanning II

Thesis submitted to the Faculty of the
Virginia Polytechnic Institute and State University
in partial fulfillment of the requirements for the degree

MASTER OF SCIENCE

in

Materials Engineering

APPROVED:

M.R. Louthan, Jr., Chairman

R.E. Swanson

N.E. Dowling

August, 1987

ABSTRACT

Acoustic emission activity resulting from plastic deformation of mild steel disks that were clamped and then pressurized from one side with either hydrogen or nitrogen was recorded and analyzed.

It was found that during monotonic pressurization of disks in nitrogen gas, more cumulative counts were recorded than for similar disks pressurized in hydrogen gas. Possible signatures of the "births" of cracks were observed during hydrogen pressurization of disks that typically failed by leaking. The records of the nitrogen tests show very high energy and high count events occurring early in the deformation process. These events are believed to be the result of the breaking away of near surface dislocations that had been pinned by nitrogen. The disks tested in nitrogen typically failed by bursting (ductile failure) while those tested in hydrogen typically failed by leaking ("brittle" failure).

Acknowledgements

The author would like to express deep thanks to his advisor, Dr. M.R. Louthan, Jr., for his support throughout this and other work. Many thanks are also extended to Drs. R.E. Swanson and N.E. Dowling for encouragement and helpful suggestions. The author would also like to thank his friends and coworkers Akmed, Bill, Ken, Mike and Ron. I must also thank Gracie for keeping me company during long nights spent in the lab (with only one "accident").

Table of Contents

| | |
|----------------------------------|-----|
| Acknowledgements..... | iii |
| List of Figures | v |
| List of Tables | vi |
| 1.0 Introduction | 1 |
| 2.0 Literature Review | 2 |
| 2.1 Disk Rupture Testing | 2 |
| 2.2 Acoustic Emission | 3 |
| 2.3 Hydrogen Embrittlement | 9 |
| 3.0 Methods and Materials | 16 |
| 4.0 Results | 21 |
| 5.0 Discussion | 22 |
| 6.0 Conclusions | 33 |
| References | 35 |
| Figures | 38 |
| Table | 62 |

List of Figures

| | |
|---|----|
| 1. Schematic of Disk Pressurizing Assembly | 38 |
| 2. Schematic of Burst and Continuous Waveforms | 39 |
| 3. Event Waveform Characteristics | 40 |
| 4. Hydrogen Embrittlement Reaction | 41 |
| 5. Microstructure of AISI 1015 Steel (125x) | 42 |
| 6. Microstructure of AISI 1015 Steel (500x) | 43 |
| 7. Graph of Cumulative AE counts vs. Gas Pressure | 44 |
| 8. Graph of Cumulative AE counts vs. Gas Pressure With Error Bars Shown For Pressurization in Nitrogen | 45 |
| 9. Graph of Cumulative AE counts vs. Gas Pressure With Error Bars Shown for Pressurization in Hydrogen | 46 |
| 10. Graph of Cumulative AE counts vs. Gas Pressure | 47 |
| 11. Graph of Cumulative AE counts vs. Gas Pressure With Notes | 48 |
| 12. Example AE Data (Energy vs. Rise Time) 200 psig ... | 49 |
| 13. Example AE Data (Amplitude vs. Rise Time) 200 psig | 50 |
| 14. Example AE Data (Energy vs. Rise Time) 250 psig ... | 51 |
| 15. Example AE Data (Amplitude vs. Rise Time) 250 psig | 52 |
| 16. Example AE Data (Energy vs. Rise Time) 950 psig ... | 53 |
| 17. Example AE Data (Amplitude vs. Rise Time) 950 psig | 54 |
| 18. Example AE Data (Energy vs. Rise Time) 1000psig ... | 55 |
| 19. Example AE Data (Ampl. vs. Rise Time) 1000psig | 56 |
| 20. Mobile Dislocation Density vs. Plastic Strain | 57 |
| 21. Schematic of Hydrogen Effects on Upper Yield Point | 58 |

22. Surface Crack on Disk Tested in Hydrogen 59
23. Fractograph of Sample That Burst in Nitrogen 60
24. Fractograph of Sample That Leaked in Hydrogen 61

List of Tables

1. Mechanical Properties of AISI 1015 Steel 62

1.0 INTRODUCTION

The presence of hydrogen is known to have very significant effects on the mechanical behavior of metals and alloys. Hydrogen can potentially cause damage in metals by weakening the lattice, interactions with dislocations, interface reactions, or by discontinuities caused by localized pressure cells. Metals may come in contact with hydrogen during pickling, plating, or heat treating operations. Hydrogen is also evolved during many corrosion processes. The most direct and obvious situation that would bring a metal into contact with hydrogen is the use of the metal as a containment vessel for the storage or transportation of hydrogen gas. Because of their relatively low cost, mild steels are likely to be used as containment vessels in future energy systems (1). Thus, characterization of the effects of hydrogen on the behavior of mild steels, including the effects of different stress states, will be important for future applications. Research in this area has been done at VPI (2,3,4,5). This thesis attempts to examine the behavior of disks biaxially stressed in a disk pressurization system using a Physical Acoustics Corporation 3104 acoustic emissions detection

system.

2.0 LITERATURE REVIEW

2.1 Disk Rupture Testing

A disk rupture test system was designed at VPI in 1977 (6). A schematic diagram of the system is shown in Figure 1. The working part of the system consists of a thick walled stainless steel plenum in which disks from 3 1/2 to 4 inches in diameter are clamped against an annulus. Pressurized gas is applied to one side of the disk, forcing it to bulge through the hole in the annulus. A convenient feature of the system is that it allows direct exposure to hydrogen (or other gas) without the need for dynamic seals or elaborate test chambers. Tests of this type have also been used by J.P. Fidelle to study hydrogen embrittlement (7). A drawback of the disk rupture test is that the pressure of the gas is not constant. This is not a problem from mechanical considerations, obviously, because the increasing pressure of gas is what is applying the load that is being used to deform the disk. However, the chemical properties of the system change as the gas pressure increases and thus the stress state and potential

for embrittlement are not independent of one another. An increase in gas pressure will result in an increase in fugacity and thus increase the probability of interaction between the gas and the metal. Also, the permeation rate of hydrogen into the metal is directly proportional to the square root of the gas pressure. This factor was not taken into account in these tests. However, since the main purpose of this thesis was to compare the behavior in hydrogen vs. nitrogen, this should not have caused any problems since the partial pressure of each gas was the same for each stage of loading.

2.2 Acoustic Emissions

The ASM Metals Handbook defines acoustic emission as "the high-frequency stress waves generated by the rapid release of strain energy that occurs within a material during crack growth, plastic deformation or phase transformation" (9). Emissions may be divided into two major types: continuous and burst. Continuous emissions have longer durations and longer rise times than burst emissions but have lower amplitudes and (frequently) lower energies. Continuous emissions have a wave form similar to Gaussian random noise and in metals are usually the result of slip within grains. Burst emissions are usually associated with

the development of micro- and macro- cracks (9), or twinning. A schematic of each type of emission is shown in Figure 2. The elastic waves propagating out from a source cause displacements on the surface of the material that can be detected and measured by means of sensitive transducers. The parameters that are recorded are defined below (10).

Acoustic Emission Event- Material change giving rise to acoustic emission. This event can be due to cracking, dislocation movement, twinning, phase transformation etc. and is detected for each material change as it occurs. This material change usually causes the acoustic emission signal to be generated in distinct packets or bursts.

Acoustic Emission Count- The number of times the acoustic emission signal exceeds a preset threshold during any selected portion of a test.

Acoustic Emission Burst- Qualitative description of acoustic emission

signals that are related to individual emission events occurring within the material.

Event Duration- A measure of time of the acoustic emission burst.

Peak Amplitude- Refers to the maximum analog signal level attained during an event or a specified period. Peak amplitude can be measured in voltage or decibels.

Rise Time- The time it takes an acoustic emission event, once detected, to reach its peak amplitude.

Acoustic Emission Energy- A relative measure of the total energy detected in a selected interval of a test. Calculated by determining the area under the acoustic emission amplitude (envelope) curve.

Acoustic Emission Envelope- A demodulated presentation of the high

frequency AE signal. The envelope "rides upon" the peak of the detected AE waveform.

Cumulative Count- Total count accumulated as a function of time.

Acoustic Emission Signature- A set of identifiable characteristics of acoustic emissions signals correlated with properties of a specific test article as observed with a particular instrumentation system under specified test conditions.

Figure 3 illustrates these parameters with an example waveform(10).

During an acoustic emissions inspection, guard sensors are usually placed around the area of interest to help eliminate noise originating from outside of this area. A "guard sensor" is a transducer strategically positioned between the area being tested and potential sources of unwanted signals. When a noise signal arrives at this transducer, the gate to the master sensor (the transducer collecting the desired data) is temporarily closed so that

the noise is not recorded by the master sensor. Guard sensors were used in this study to eliminate noise from the sounds of valves opening and closing, as well as any other unwanted noise originating from other parts of the system.

The earlier advancements in AE studies are attributed to the work of Kaiser (11). In his work, the irreversible nature of AE, now known as the "Kaiser Effect", was first studied. It states that after a metal has been loaded and unloaded, no further acoustic activity occurs during reloading until the previous maximum load has been exceeded. In the mid 1970's enthusiasm for using acoustic emissions as a reliable nondestructive test technique was very high, but laboratory results showed that tough steels could undergo deformation and cracking with no acoustic emission activity being generated (12). However, numerous improvements in the detection techniques have been made since then.

Acoustic emission signals are currently being used to study various phenomena and to nondestructively test numerous structures. They have been used to study plastic deformation, crack initiation, and crack propagation in engineering materials (13,14).

One area of interest has been the assessment of fatigue damage. Correlations have been made between cumulative counts and counts/cycle vs. the number of cycles. Bassim has found acoustic emissions to be effective

for monitoring the fatigue of structural (1015,4340) steels and has derived relationships between total counts per cycle and ΔK (15). AE have also been used to study crack closure, where it was found that the closing of a crack in aluminum alloys and 304 stainless steel resulted in a distinct AE signal that differed from the signal resulting from crack extension (16). Monitoring of corrosion fatigue revealed that the AE activity depended on crack size and crack surface deposits (17). Acoustic emissions detection is very useful for the continuous monitoring the propagation of a fatigue crack (18).

Investigations are currently being made of the usefulness of AE for nondestructively evaluating the integrity of structures such as pressure vessels, aircraft components, storage tanks, offshore rigs, and highway bridges. The feasibility of using acoustic emissions to detect leaks from stress corrosion cracks in the piping of light water reactor plants in the U.S. has been studied and AE leak detection programs are expected to be implemented (19,20,21). Acoustic emissions are useful for performing hydrotests on pressurized power plant components because the real time data analysis provides an early warning of potential catastrophic failure (22). Numerous attempts for in flight monitoring of aircraft structures have been made, but actual applications are still in the developmental stage (23,24,25,26). Methods for using AE to detect leaks

in atmospheric liquid hydrocarbon storage tanks have been successfully developed and will aid in meeting environmental protection requirements (27). Attempts to monitor very large structures such as highway bridges and oil rigs have met with only limited success so far, but research is progressing (27,28). The main problems with large structures are attenuation and mechanical noise. Appropriate band pass filtering should eventually make the rejection of noise possible (29). However, problems with attenuation still exist because the high frequency components of the signals (those components that are left after filtering of the noise) attenuate very rapidly and can only be detected if the transducer is relatively close to the crack (30).

2.3 Hydrogen Embrittlement

It has been said of the literature on hydrogen embrittlement that "The literature pertaining to the effects of hydrogen gas on the plastic properties of iron and steel is extensive, contradictory, and confusing" (3). That was ten years ago, but today the literature is even more contradictory and confusing. There are numerous theories and many of them directly conflict with one another. A quote from a poem by S.P. Rideout sheds light on

another common aspect of the literature (31):

At intervals researchers gather,
And on mechanisms palaver;
Each to his own work will refer,
Ignoring those who don't concur.

How true the above statement is. Researcher after researcher develops theories based on other theories (usually their own) that are still unproven or in conflict with other experimental evidence. The crux of the problem is that environmentally assisted cracking is a very complicated process. Overall mechanisms must combine numerous smaller scale phenomena that frequently are not completely understood themselves. Some variables that affect hydrogen assisted cracking include time, stress level, stress state, temperature, pressure, physical state of the environment, microstructure, hydrogen concentration, surface conditions, and mechanical properties.

The first step in hydrogen embrittlement is that the metal must be exposed to hydrogen. This is perhaps the only aspect of hydrogen embrittlement that is not in dispute. A metal can contact hydrogen in a multitude of ways. Any time iron comes in contact with liquid water or water vapor the

potential exists for absorption of hydrogen by means of chemical reaction with or dissociation of water molecules. Anything that promotes chemical reaction with water, such as low pH, high temperatures, or electrical current will potentially increase the availability of hydrogen to the metal (but will not necessarily increase the potential for hydrogen embrittlement because other factors - such as solubility and diffusivity - may be affected). Welding with water present, cathodic charging during electroplating, heat treatments, and acid pickling are just a few of the processes that may enable metals to absorb hydrogen from water. General corrosion also results in the production of hydrogen, which may lead to embrittlement. Thus, stress corrosion cracking of steels and hydrogen embrittlement of steels are frequently interrelated. All of the above involve hydrogen from moisture. Obviously, a metal may also absorb hydrogen directly from gaseous hydrogen.

The hydrogen must somehow diffuse into the metal in order to have a deleterious effect. The first step in this process is physical adsorption. This occurs most readily on a clean metal. Other gases, particularly oxygen, may preferentially adsorb on the surface. Thus the potential for hydrogen embrittlement is usually reduced in the presence of oxygen (32,33,34). On the surface of the metal the hydrogen molecule can dissociate into hydrogen atoms, also known as nascent hydrogen. Because of their small

size, hydrogen atoms are capable of diffusing rapidly into the iron. Figure 4 schematically illustrates this process. It is generally agreed upon that hydrogen uptake by steels increases as deformation occurs (7,35,36,37,39). It is quite likely that dislocations increase the transport of hydrogen into the metal (37) and the diffusion of hydrogen assisted by dislocation motion is probably several orders of magnitude greater than ordinary lattice diffusion (33).

Thus far it has been stated that for hydrogen embrittlement to occur a susceptible metal must come in contact with hydrogen, the hydrogen must physically adsorb and dissociate on the surface, and the hydrogen must diffuse into the metal. After the hydrogen has diffused into the metal, how does embrittlement occur? This is where the serious confusion begins. In the remainder of this literature review, a brief discussion of the history of hydrogen embrittlement theories will be given.

In the early 1940's, C.A. Zapffe et al. introduced the idea of the "planar pressure theory" (40,41). In a 1941 paper, Zapffe (41) discusses at length the necessity that a defect substructure must exist in metals in order to be able to explain changes in phenomena such as mechanical yielding, thermal and electrical conductivity, crystal growth, and hydrogen assisted cracking. Scientists of that era expended a great deal of effort arguing whether such structures were random or ordered if they existed at all.

Each could cite valid experimental evidence to prove their own theories. Of course, these "defect substructures" do exist and are now explained by modern dislocation theory. Both the random theory supporters and ordered theory supporters were probably somewhat right, since dislocation phenomena have both random and ordered aspects depending on metallurgical variables. Zappes in his planar pressure theory proposed that hydrogen embrittlement occurred because a pressure developed in the steel at "interblock disjunctions" (it is not entirely clear what these were supposed to be). The theory stated that this pressure increased until it eventually exceeded the elastic limit and "sprung the material apart" to produce the observed flat fracture features. Although relatively crude, some of the elements are the same as those used twenty years later by Troiano.

Studies by Bastion and Azou (42) in the early 1950's confirmed that hydrogen had little effect on the flow properties of iron and steel but did significantly lower the true fracture stress and true fracture strain. They also studied the strain rate sensitivity of embrittlement and found that the degree of embrittlement decreased with increasing strain rates. It was also found that dislocation transport processes were important to localization of hydrogen.

N.J. Petch and P. Stables (43) proposed a mechanism

based on Griffith's crack theory that said hydrogen could lower fracture stress by diffusing to the crack tip and then lowering the surface energy through adsorption. A major problem with this theory is that it ignores plasticity.

A.R. Troiano's 1960 paper provided the foundation for the weakened lattice model for hydrogen embrittlement (44). Troiano stated that hydrogen embrittlement - or, more specifically, slow strain rate embrittlement - takes place by the same mechanism as strain aging embrittlement. This is saying that hydrogen behaves in a manner similar to the behavior of other interstitials such as carbon, nitrogen, oxygen, and boron, with the main difference being the operative temperature ranges. His theory is that the lattice of iron and other transition metals is weakened by the additions of solutes that tend to fill the 3d orbital. This lowers the strength of the lattice and thus facilitates cracking. An important aspect of Troiano's paper is that consideration is beginning to be given to the interactions between hydrogen and individual lattice atoms.

C.D. Beachem in 1972 developed a "hydrogen embrittlement" model that said hydrogen wasn't embrittling at all, but was facilitating whatever deformation processes would normally take place in the specific alloy (45). In contrast to models that said hydrogen locks dislocations in

place, Beachem's model stated that hydrogen unlocks them. However, his theory does support the idea that hydrogen atoms are locked in place by deformation. This is where a weakness in the model may be found. If hydrogen atoms are locked into place by dislocations, would not the reciprocal (that is, hydrogen locks dislocations into place) also have to be true from irreversible thermodynamic considerations? In any case, Beachem's model fits a wide range of experimental observations and it is this model that is believed to best fit some of the experimental data of this thesis.

The earliest known recorded study of hydrogen embrittlement was by W.H. Johnson in 1873 (46). Johnson observed that iron wires showed a loss of ductility after a brief immersion in strong hydrochloric or dilute sulphuric acid. Johnson made several conjectures about hydrogen embrittlement that other researchers later found to be true, such as the high diffusivity of hydrogen in steel, the importance of surface condition to susceptibility to embrittlement, and that general corrosion could lead to hydrogen embrittlement. He also noted that wires were not embrittled when exposed to hydrogen gas and then tested in air. Later researchers found that mild steels had to plastically deformed in the hydrogen gas for embrittlement to occur. But Johnson could never have developed this theory because in 1873 no one knew about dislocations in

metals. Although Johnson - whether through intelligent insight or lucky guesses - was headed in the right direction, the fact remains that he made numerous blunders in his reasoning that were not due to stupidity but to the inavailability of more sophisticated testing equipment and more sophisticated theories of the structure of matter. The point being made here is that perhaps researchers of the future will reflect on all of the current theories of hydrogen embrittlement and see in what way scientists stumbled on to correct and incorrect theories.

3.0 METHODS AND MATERIALS

A disk pressurization system was used to pressurize disks of 1015 steel in the environment of interest. A schematic diagram of the assembly is shown in Figure 1. Monotonic pressurization tests involved increasing the gas pressure on the disk, which resulted in bulging of the disk. Acoustic emission data were recorded on a floppy disk for each 50 psi increment of pressure. The inner radius of curvature of the clamping washer is large enough that the biaxial state of stress developed at the center of the disk is higher than the stresses developed in the clamped area. When the disk is bulged to a hemispherical shape the in-plane shear stresses approach zero and thus the lattice dilation is greater than for most other types of loading,

such as uniaxial and non-equibiaxial. This condition frequently increases susceptibility of some metal alloys, such as mild steels, to hydrogen embrittlement (2) . Previous studies at VPI on mild steels (2) have found from disk rupture tests that hydrogen promotes a leak before burst mode of failure, while oxygen pressurization promotes failure by bursting. Samples that leaked in hydrogen failed in a brittle manner by cracking along the plane of maximum tensile stress, while samples that burst in oxygen (and also nitrogen) failed in a ductile manner by means of microvoid coalescence along the plane of maximum shear stress.

Disks were .04 cm thick and were made of hot-rolled spheroidized AISI 1015 steel. The uniaxial mechanical properties are listed in Table 1. The microstructure of the steel is shown in Figures 5 and 6. For acoustic emission monitoring a Physical Acoustics Corporation 150 kHz piezoelectric transducer was attached to the plenum. An effort was made to keep constant all factors that might alter acoustic emission signals so that differences observed between the different gases would be the result of actual differences in behavior rather than differences in the way the AE signals were detected. Because the disk was clamped very tightly in the plenum, it may be assumed that AE signals were capable of easily propagating from the disk to the plenum to the transducer. It is to be expected that

the signals detected through the plenum may be different from signals that would have been detected had the transducer been attached directly to the disk (which could not be done because of bending of the disk). However, for the purpose of comparing signals from tests using different gases it may be assumed that each signal will be modified in a similar manner and thus an accurate comparison can still be made. Another possibly important factor is the anisotropy of the disks, which had a texture as a result of being cut from rolled sheet. To make results as consistent as possible the transducer was always positioned at the same spot on the plenum and the disk was always inserted with the rolling direction the same relative to the transducer.

Another consideration was the possibility of noise from the pressurizing gas. Nitrogen was much more likely to be a problem because it has a viscosity twice as great as the viscosity for hydrogen. A critical experiment to measure the level of gas noise involved bulging a disk to about 1550 psig (approximately 100 psig less than the typical failure pressure) then depressurizing and repressurizing the disk several times until no emissions were detected. The fact that any signals at all were detected during repressurization indicates that fatigue damage was occurring. The Kaiser effect is not observed in such situations. However, after several cycles this noise

disappeared completely. Thus, since it was possible to fill the volume of the disk without detecting any noise, it may be concluded that there was no gas noise at the rates of pressurization that were used.

Another potential source of noise may have been sliding of the disk against the clamping washer as the load was applied. To check for such noise, the bulged disk from above was removed from the plenum and then reclamped into the plenum. No acoustic emission activity was detected during reloading, so it may be concluded that the total background mechanical noise was below the threshold of detection.

Disks were pressurized in 50 psi increments at the rate of about 100 psi per minute. Attempts were made to keep the pressurization rate as constant as possible because other work has shown the level of acoustic emissions activity to be sensitive to strain rate because of changes in the mobile dislocation density (47). Acoustic emission data for each 50 psi increment were stored for future plotting and analysis. The AE detection system stored the following parameters: counts, cumulative counts (vs. time), energy, cumulative energy (vs. time), amplitude, rise time, events, and duration. The software from Physical Acoustics Corporation was capable of plotting any of the above parameters against any of the other parameters. From these data curves of cumulative counts vs. pressure were

calculated for each gas (Figure 7). Figures 8 and 9 give the same plot but include error bars of plus or minus one standard deviation. Figure 10 is a plot of the original data points used to calculate the curves in Figure 7. To compare and analyze the various parameters, the following ratios were calculated: energy/rise time, energy/duration, and amplitude/rise time. Example printouts of the parameters at selected gas pressures are shown in Figures 12 through 19.

4.0 Results

For 1015 mild steel disks tested in the disk pressurization system it was found that cumulative acoustic emission counts was significantly higher when nitrogen was used as the pressurizing gas than when hydrogen was used as the pressurizing gas, as shown in Figure 7. At various stages of deformation with each gas there were distinct acoustic emission signatures. During the initial part of deformation in nitrogen very high acoustic emission events were detected. Figure 12 compares energy vs. rise time for pressurization in hydrogen or nitrogen at 200 psig. Figure 13 contains the same data, but plotted as amplitude vs. rise time. Figures 14 and 15 compare energies and amplitudes recorded at a gas pressure of 250 psig. Note that high energy events occurred during the early stages of pressurization in nitrogen but not during the early stages of pressurization in hydrogen. In the 900-1100 psig (56% to 69% of failure pressure) region of pressurization burst emissions with brittle crack signatures were observed for samples that failed by leaking in hydrogen but similar emissions were not detected during pressurization in nitrogen until above 1200 psig. Figures 16 through 19 illustrate typical signatures for hydrogen cracking. The events from cracks have high energies, low rise times, and high amplitudes. Note that the high energy events recorded

during the early part of the deformation in nitrogen had relatively long rise times. Figure 11 summarizes the observations that were made.

Pressurization in hydrogen promoted failure by leaking while pressurization in nitrogen promoted failure by bursting. Seven out of ten disks tested in hydrogen leaked and nine out of ten samples tested in nitrogen burst. The average failure pressure was 1575 psig in hydrogen and 1650 psig in nitrogen.

5.0 Discussion

The types of AE emission observed may be divided into three general categories: very high energy events, high energy events, and background events.

The observation of very high energy events early in the deformation in nitrogen gas can perhaps best be explained in terms of a pinning effect of carbon or nitrogen on dislocations. The part of the curve referred to here is indicated in Figure 11. It has been established that most of the dislocations in a deformed metal are concentrated near the surface because dislocation nucleation is easier at a free surface. It is possible that nitrogen diffused into a thin surface layer of the metal - where most of the dislocations are concentrated -

enough to interact with and pin dislocations. Studies by Marcus (48) show that metals in an oxygen environment (as opposed to metals in a vacuum) develop a significantly high (high enough to increase the fatigue crack growth rate) concentration of dissolved oxygen near the surface. Although Marcus' results involved oxygen in iron, it is not unreasonable to assume that nitrogen would be at least as likely as oxygen to diffuse into steel because nitrogen atoms are only slightly larger than oxygen atoms. Also, nitrogen is lighter than oxygen and diffusivity is proportional to the inverse of the square root of the atomic mass. Furthermore, since nitrogen has a higher solubility and diffusion coefficient than carbon it would be expected that nitrogen can potentially have a significant role in dislocation interactions. Thus, the proposed explanation is that atoms of nitrogen from the high pressure nitrogen gas diffuse into the surface of the metal where most of the dislocations are concentrated and then pin dislocations. Thus, it is possible that the breaking away of dislocation pileups caused the observed high energy events.

The curve of counts vs. nitrogen gas pressure shows a decrease in slope at a pressure of about 300 psig, as may be seen in Figure 11. This can best be explained in terms of changes in the mobile dislocation density. As plastic deformation proceeds the total dislocation density

increases. The increasing number of dislocations is the means by which flow occurs, but as the population density increases flow begins to be hindered by interactions between dislocations. There are two ways of describing the effects of interactions on the mobile dislocation population (49). One approach assumes that the average dislocation velocity decreases with increased plastic strain because of an increasing number of collisions and the other approach assumes that dislocations continue to move at the same velocity but the fraction that is mobile decreases with increasing strain. The two approaches are statistically equivalent. Using the approach that the mean velocity remains constant, the curves shown in Figure 20 may be developed. Figure 20c can readily be used to explain the change of slope at 300 psig of the curve for pressurization in nitrogen. This part of the curve is indicated in Figure 11. This change in the slope is probably the result of the near surface region of the disk exceeding its peak density of potentially mobile dislocations. After a certain density is reached, many dislocations become immobilized by becoming entangled with other dislocations, and breakaways become less common. A similar argument may be used to explain the change of slope that occurs at about 300 psig in the curve for pressurization in hydrogen gas.

There are several possible ways to attempt to explain

the lower AE count level observed during pressurization in hydrogen. Following a line of reasoning similar to the one used above, the behavior can most easily be explained in terms of hydrogen not pinning dislocations in the same manner that nitrogen pins dislocations. This correlates well with the mechanical yield point suppression of a-106 steel observed by Sudarshan et al. (50). This phenomenon is illustrated in Figure 21. The suppression of the yield point is the result of the same mechanisms that are causing the high energy events to be absent during the early stages of pressurization in hydrogen gas. That is, hydrogen is competing with the carbon or nitrogen atmospheres for positions along the dislocation lines. Apparently, dislocations do not break away from hydrogen atmospheres the same way they do from carbon or nitrogen atmospheres. Freely moving dislocations give rise to low amplitude, low energy events compared to the breaking away of pinned dislocations, which give rise to higher energy, higher amplitude events. Although considerable evidence has been accumulated in support of an enhanced dislocation model (45,51,52,53), there are still, of course, many factors still in dispute. It might be possible that hydrogen can induce dislocation motion by generating a large enough potential field to overcome the Peierls-Nabarro stress holding the dislocation in place. Ficalora (51) has shown through resistance measurements on bcc iron that hydrogen

in the lattice can increase the number of dislocation sources activated during deformation. A piece of evidence against this model is that no conclusive observations of macroscopic softening are available. This might be expected to occur if hydrogen were truly facilitating dislocation motion. Another important piece of information is that plastic deformation (dislocation motion) greatly increases the diffusion of hydrogen into the steel. There are several possible ways of interpreting this observation. If hydrogen moves with dislocations then it would seem possible that hydrogen might hinder dislocation motion in a manner similar to the way other impurity atmospheres (C, O, N, for example) hinder dislocation motion. However, other lines of reasoning could be followed to support the idea that hydrogen enhances dislocation motion by interacting with a dislocation in a manner that lowers the stress field holding the dislocation in place. The possibility also exists for yet another phenomenon to occur. It has been observed that grain boundaries can migrate when substitutional or interstitial atoms diffuse more rapidly along grain boundaries than through the lattice. Li et al. (51) have proposed a mechanism based on free energy changes of mixing that says solutes can move dislocations if diffusion of the solute is more rapid along the dislocations than through the lattice. Another important fact is that hydrogen decreases the response to

strain (or stress) aging. Studies on 304 stainless steel showed that the stress aging effect was virtually eliminated after cathodic charging in hydrogen (54). This appears to support the idea that hydrogen is not pinning dislocations in place.

However, since no one truly knows the nature of the local strain field of a dissolved hydrogen atom, there is no way to reach a firm conclusion about the manner in which hydrogen affects dislocation motion. Perhaps someday new microscopy techniques that are capable of resolving distances almost of atomic size, such as those based on electron tunneling, will enable scientists to clarify the interactions between dissolved hydrogen and metal lattices.

The curve for cumulative counts in hydrogen shows a rise at about 900 psi. This is also the region where high energy crack-like burst emissions were detected, as indicated in Figure 11. Examples of these signatures are given in Figures 16 through 19. Note that the characteristics that are assumed to be the result of cracking are high energy, a high energy to rise time ratio, and a high amplitude to rise time ratio. The ratio of energy to duration was found to be a constant for almost all of recorded events. The burst emissions typically occurred between 900 and 1150 hydrogen gas pressure and then ceased. For the remainder of the deformation the cumulative AE counts rose linearly with pressure. It is

believed that the observed burst emissions are the result of microcracks of a critical size being created, as is indicated in Figure 11. The gas pressure at which this inflection point occurs could potentially be used for evaluating the effectiveness of hydrogen embrittlement inhibitors. It would be expected that an effective inhibitor would shift the inflection point to a higher gas pressure.

The idea that a crack must be born a certain minimum size or larger arises from surface energy and strain energy considerations. When a material is strained, energy is stored in the material. If this strain energy is released, the energy state of the material is lowered. Thus, the release of strain energy is the driving force for a crack to nucleate. For simplicity, assume a symmetric elliptical crack of length $2c$ is being formed. The Inglis solution for strain energy release from such a crack is

$$U_d = \frac{2\pi\sigma^2 c^2}{E}$$

where U_d is the strain energy, c is the crack half-length, σ is the applied stress, and E is the Young's modulus. However, the nucleation of a crack involves the creation of two new surfaces. The energy required to form the new surfaces is

given by

$$U_s = 4 \gamma c$$

where U_s is the energy to form the surface and is the γ surface energy per unit area. The net energy change is equal to the sum of the above two equations. The maximum in the curve for total energy corresponds to c^* , the critical crack size. This is the minimum size for which energy considerations favor the birth of a crack. The acoustic emissions data appear to be indicating that at a gas pressure of about 950 psig cracks are able to be born. Above about 1150 psig, no further burst emissions occur during pressurization in the hydrogen gas. Figure 22 is a crack on the surface of a disk pressurized to 1500 psi in hydrogen. The birth of this crack was detected as a single burst emission at a gas pressure of 1000 psi. The crack as shown here has nearly grown to penetrating size.

Crack-like emissions were also detected in nitrogen, but detection of these usually began at considerably higher gas pressures (1250 psig in nitrogen vs. 900 psig in hydrogen). Figure 23 shows the fracture surface of a sample that failed by bursting in nitrogen. Microvoids are the predominant feature and thus the macroscopic mode of

failure was ductile. Figure 24 shows the fracture surface of a sample that leaked in hydrogen. The fracture surface is similiar to other fracture surfaces where the macroscopic failure mode was found to be quasicleavage (5). Thus, it would seem that a reasonable interpretation of the data is that hydrogen is lowering the strain (or stress) at which cracks begin to form.

A possible mechanism by which hydrogen may be facilitating the nucleation of cracks is the precipitation of gaseous hydrogen at internal defects. This theory is based on the fact that hydrogen diffuses much more rapidly when aided by dislocations than it does through the lattice alone. Thus, pressure may build up at voids in the material when hydrogen is transported to the voids by dislocation motion faster than it can escape by diffusion.

As with all other embrittlement models, the internal pressurization model is subject to considerable debate. But in any case, evidence that this may have occurred may be seen in Figure 24. Note the separation of the inclusions from the iron matrix. However, even if the internal pressurization phenomenon did occur, this alone might not be sufficient to account for the overall quasicleavage appearance of the fracture surface.

The mechanism that appears to best fit the experimental observations is that proposed by Beachem (45).

This model accounts for the lower observed AE activity, the earlier births of cracks, and the changes in macroscopic failure mode. Beachem's argument is that all fracture occurs by plastic processes, with only variations in the concentration and form of plasticity, that hydrogen aids this plasticity, and the plasticity, in turn, facilitates the movement of hydrogen to the critical portion of the material.

It is proposed that either this phenomenon was solely responsible for the experimental observations or that it occurred in conjunction with the previously discussed nitrogen stress aging effect.

The main idea behind Beachem's model is that hydrogen dissolved in the lattice in the vicinity of the crack tip will aid whatever deformation processes would normally occur anyway. This is saying that macroscopically "brittle" fractures are actually the result of very small scale plasticity. An inherent part of this theory is that hydrogen must make the movement or generation of dislocations more easy. This idea fits well with the experimentally observed decrease in the AE count levels.

This mechanism would also explain why it would be easier to nucleate a crack. In ductile materials, such as mild steels, microcracks or microvoids are usually nucleated at stress concentrations resulting from dislocation pile-ups. If the increased local plasticity

model is true, one would expect that once a pile-up began it would continue to form at an increased rate because the hydrogen content would increase (through dislocation transport) and the increased hydrogen content would increase the mobility of or number dislocations and thus increase the pile-up. In this manner, it may be possible for dissolved hydrogen to stabilize a microcrack.

To summarize the items discussed above, refer to Figure 11. As deformation proceeds from a gas pressure of zero to a gas pressure of 300 psig, very high energy events are observed for the nitrogen gas but not for the hydrogen gas. These events are the result of the breaking away of groups of dislocations from carbon or nitrogen atmospheres. In the hydrogen gas, the hydrogen competes with carbon or nitrogen for sites along the dislocation line. Dissolved hydrogen results in an absence of the very high energy events caused by dislocation breakaways. In the range of approximately 900-1000 psig in hydrogen, high energy events resulting from crack initiation are observed. These events may be distinguished from the very high energy events that occurred early in the deformation in nitrogen because the hydrogen cracking events have a higher energy to rise time ratio. There is a linearly increasing region in hydrogen gas after 900 psig that is a result of crack propagation.

Currently, the use of acoustic emission detection as a nondestructive evaluation technique is limited by the

inability to distinguish between different types of phenomena occurring in a material. Acoustic emission data tells one that something has happened, but not what has happened. Studies such as this thesis illustrate the possibility of distinguishing between different phenomenon, such as dislocation breakaway vs. microcracking, based on waveform characteristics.

6.0 Conclusions

When AISI 1015 steel disks are plastically deformed by means of a disk pressurization system, the resulting acoustic emission activity is dependent on whether hydrogen or nitrogen is used as the pressurizing gas. Pressurization with nitrogen gas results in a higher level of cumulative counts than does pressurization with hydrogen gas. This is believed to be the result of interactions between the gaseous environment and the dislocation structures of the steel. It is possible that the higher AE count level observed for pressurization with nitrogen was the result of the breaking away of pinned dislocations. Pressurization in hydrogen resulted in a decreased failure pressure and tended to change the failure mode from bursting to leaking. This is believed to be the result of hydrogen lowering the stress at which a crack will nucleate. The mechanism for

this is not clear, but it was proposed that hydrogen enhanced the small scale plasticity at the crack tip. By means of the acoustic emissions detection system, it was possible to distinguish between dislocation related events and crack formation.

References

1. M. Newman, J. Grey, eds., Utilization of Alternative Fuels for Transportation, American Institute of Aeronautics and Astronautics, New York, 1979.
2. R.P. McNitt, R.D. Sisson, M.R. Louthan, Jr., B.A. Lewis, J. Murali, and J. Wagner, Hydrogen Effects in Metals, ed. I.M. Bernstein and A.W. Thompson, Carnegie-Mellon University, 1981.
3. J. Murali, Effects of Hydrogen on the Deformation and Fracture of High and Low Strength Steels, Ph.D Thesis, VPI, 1980.
4. J. Wagner, Hydrogen Embrittlement, M.S. Thesis, VPI, 1982.
5. B.A. Lewis, Role of Surface Finish in Hydrogen Embrittlement of Mild Steels, M.S. Thesis, VPI, 1982.
6. J. Masters, Disk Rupture Testing for Hydrogen Embrittlement, M.S. Thesis, VPI, 1977.
8. M.R. Louthan, Jr., G.R. Caskey, Jr., J.A. Donovan, Mater. Sci. Eng., 10, 1972.
9. Metals Handbook, 8th Edition, vol. 11, Nondestructive Testing and Quality Control, American Society for Metals, Metals Park, Ohio, 1976, pp. 234-243.
10. Physical Acoustics Corporation, User's Manual, Princeton, NJ, 1981.
11. V.N. Kudryautsev, Kh.G. Schmitt-Thomas, W. Stengel, Corrosion, 37, No. 12, Dec. 1981.
12. H.N. Wadley, J.A. Simmons, Review of Progress in Quantitative Nondestructive Evaluation, 3B, 683-697.
13. M.N. Bassim, M. Veillette, Mater. Sci. Eng., 50, 1981, 285-287.
14. K.N. Tandon, K. Tangri, Mater. Sci. Eng., 20, 1975, 47-54.
15. M.N. Bassim, M. Houssny-Evan, J. Acoust. Emiss., Apr-Sept, 4, 1985.
16. G. Lu, Ibid.

17. C. Thaulow, Ibid.
18. S.K. Pathak, C.R. Murphy, Ibid.
19. W.F. Hartman, Ibid.
20. T.N. Claytor, D.S. Kupperman, Ibid.
21. D.S. Kupperman, Ibid.
22. G. Tonolini, G. Villa, Ibid.
23. P.H. Hutton, Ibid.
24. G.G. Martin, I.G. Scott, Ibid.
25. C.R. Murphy, M.A. Majeed, S.C. Pathek, A.K. Rao, Ibid.
26. S.L. McBride, J.W. Maclachlan, Ibid.
27. P. Tschenesing, Ibid.
28. R. Visweswaran, M. Manoharan, G. Jothinathan, Ibid.
29. D.W. Prine, T. Hopwood, Ibid.
30. A. Ghobanpoor, D.W. Vannoy, Ibid.
31. R.P. McNitt, M.R. Louthan, Jr., eds., Environmental Degradation of Engineering Materials, VPI, Blacksburg, VA, 1977.
32. G.G. Hancock, H.H. Johnson, Trans. TMS-AIME, 1965, 236, 513-516.
33. J.P. Hirth, Met. Trans., 1980, 11A, 861-890.
34. D.P. Williams, P.S. Pao, R.P. Wei, Environment-Sensitive Fracture of Engineering Materials, ed. Z.A. Fornoullis, AIME, 1979.
35. P. Bastien, P. Azou, C.R. Acad. Sci. Paris, 1951, 232, 1845-1848.
36. J. A. Donovan, Met. Trans. A, 1976, 7A, 145-149.
37. M.R. Louthan, Jr., G.R. Gaskey, Jr., J.A. Donovan, D.E. Rawl, Mater. Sci. Eng., 1972, 10, 357-368.
38. J.P. Fidelle, R. Brouder, C. Pirroriani, C. Roux,

- "Disk Pressure Technique", ASTM STP 543, June 1972.
39. M. Kurkela, R.M. Latanision, Scr. Met., 13, 1979, 927-932.
40. C.A. Zappfe, M.E. Haslem, Metals Technology, 13, No. 1, 1-28, Jan. 1946.
41. C.A. Zappfe, C.E. Sims, Trans. AIME, 145, 225-261, 1941
42. P. Bastien, P. Azou, Proceedings of the First World Metallurgical Congress, ASM, 1951.
43. N.J. Petch, P. Stables, Nature, 169, May 1954.
44. A.R. Troiano, Trans. ASM, 52, 1960.
45. Beachem, C.D., Met. Trans., 3, Feb 1972.
46. W.H. Johnson, Proceedings of the Royal Society of Society, 23, 1875.
47. A. Paweek, W. Stryjewski, W. Bochniatl, H. Dybiec, Trans. Jpn. Inst. Met., 1985, 26, (9), 622-629.
48. H.L. Marcus, Environmental Degradation of Engineering Materials, ed. M.R. Louthan, Jr., R.P. McNitt, 1977, 41-54.
49. J.J. Gilman, Micromechanics of Flow in Solids, McGraw-Hill, 1969, 195-197.
50. T.S. Sudarshan, M.R. Louthan, Jr., R.P. McNitt, Scr. Met., 12, 1978, 799-803.
51. M.V. Rodriguez, P.J. Ficalora, Scr. Met., 1986, 20, 621-625.
52. J.C. Li, C.G. Park, S.M. Ohr, Scr. Met., 1986, 20, 371-376.
53. R. Gibala, Trans. AIME, 234, 1967, 1574.
54. M.R. Louthan, Jr., Status Report Sept 1, 1964, Savannah River Laboratory, Aiken, SC.

SCHEMATIC OF DISK PRESSURIZING ASSEMBLY

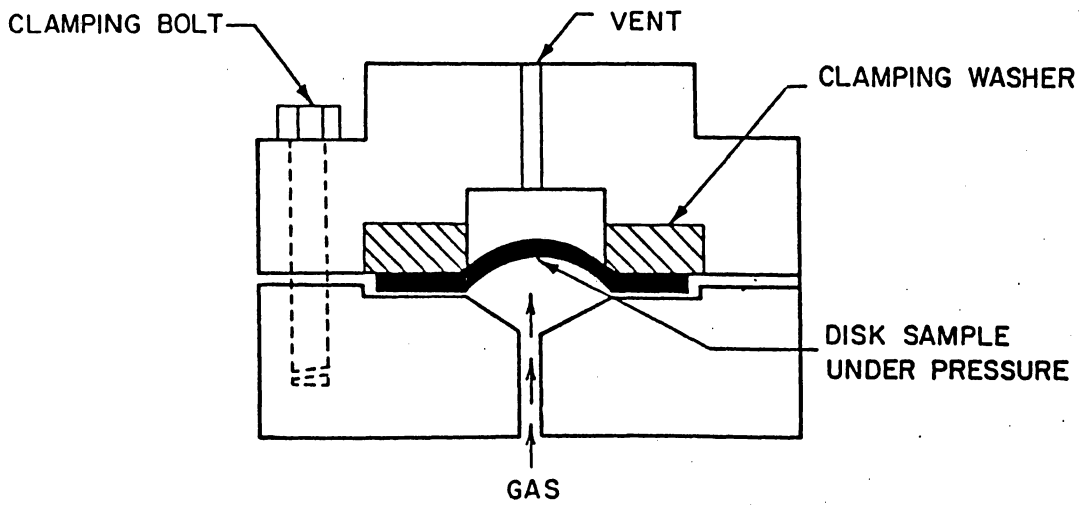


Figure 1

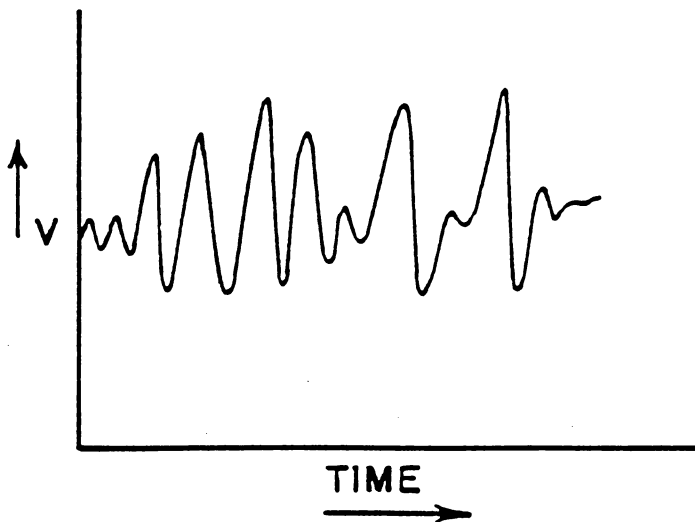
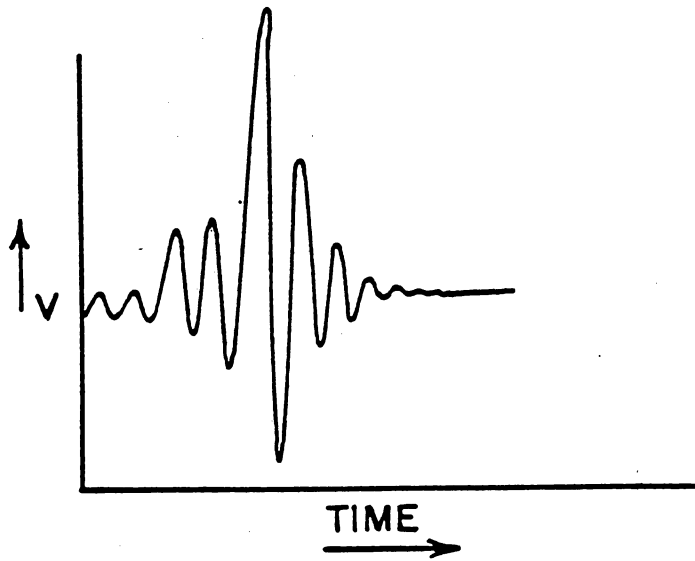
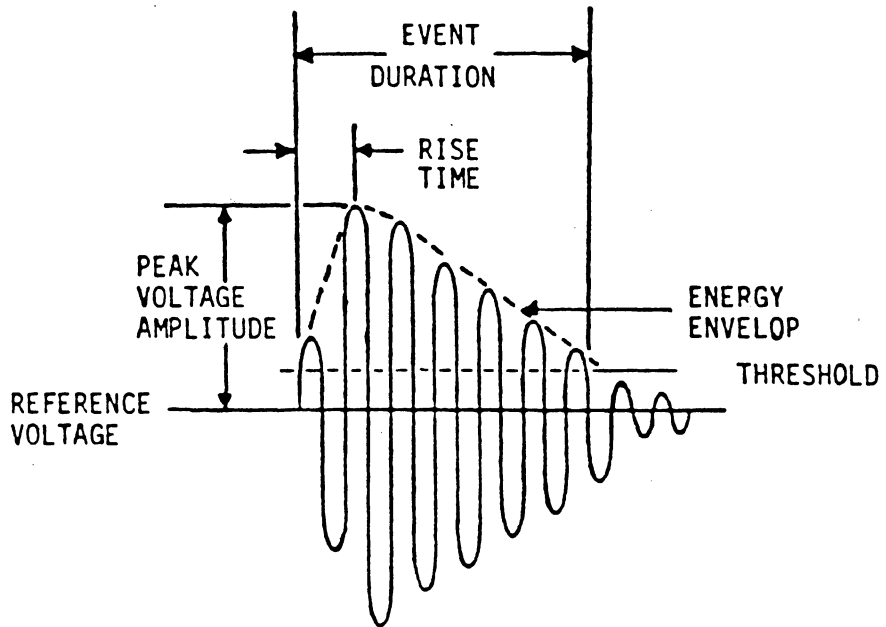


Figure 2. Schematic of burst (top) and continuous (bottom) acoustic emission waveforms (10).



EVENT WAVEFORM CHARACTERISTICS

COUNTS (EXAMPLE 7 COUNTS)
 AMPLITUDE (EXAMPLE 66 dB)
 DURATION (EXAMPLE 361 μ s)

Figure 3. Example waveform illustrating common AE terms (10).

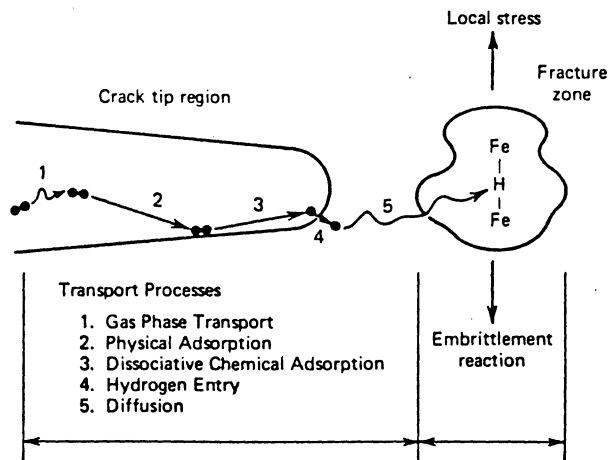


Figure 4. Various processes involved in the hydrogen embrittlement of ferrous alloys (34).

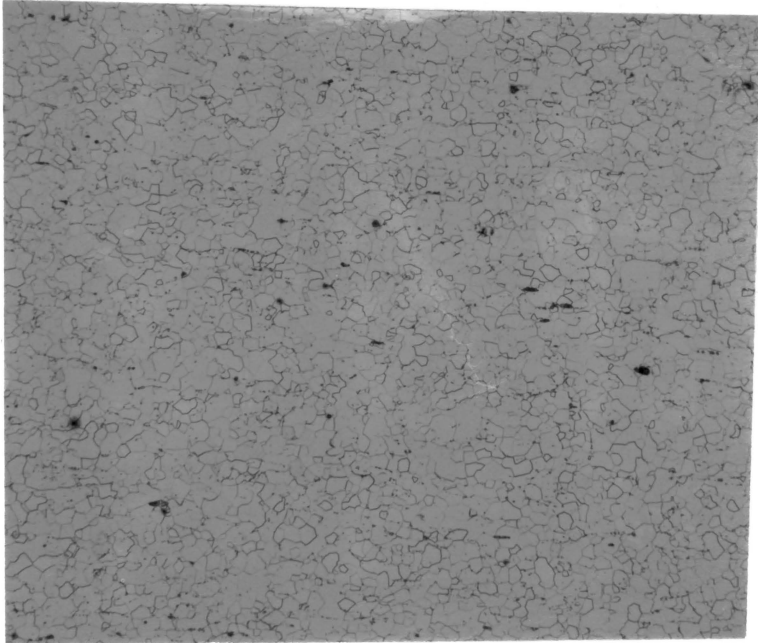


Figure 5 . Microstructure of AISI 1015 steel (125X).

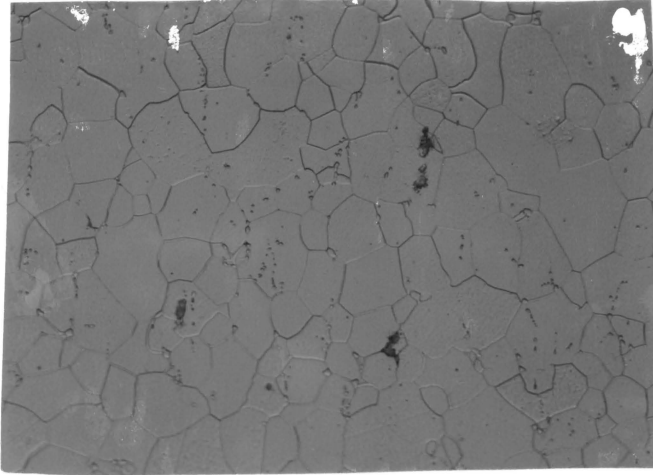


Figure 6 . Microstructure of AISI 1015 steel (500X).

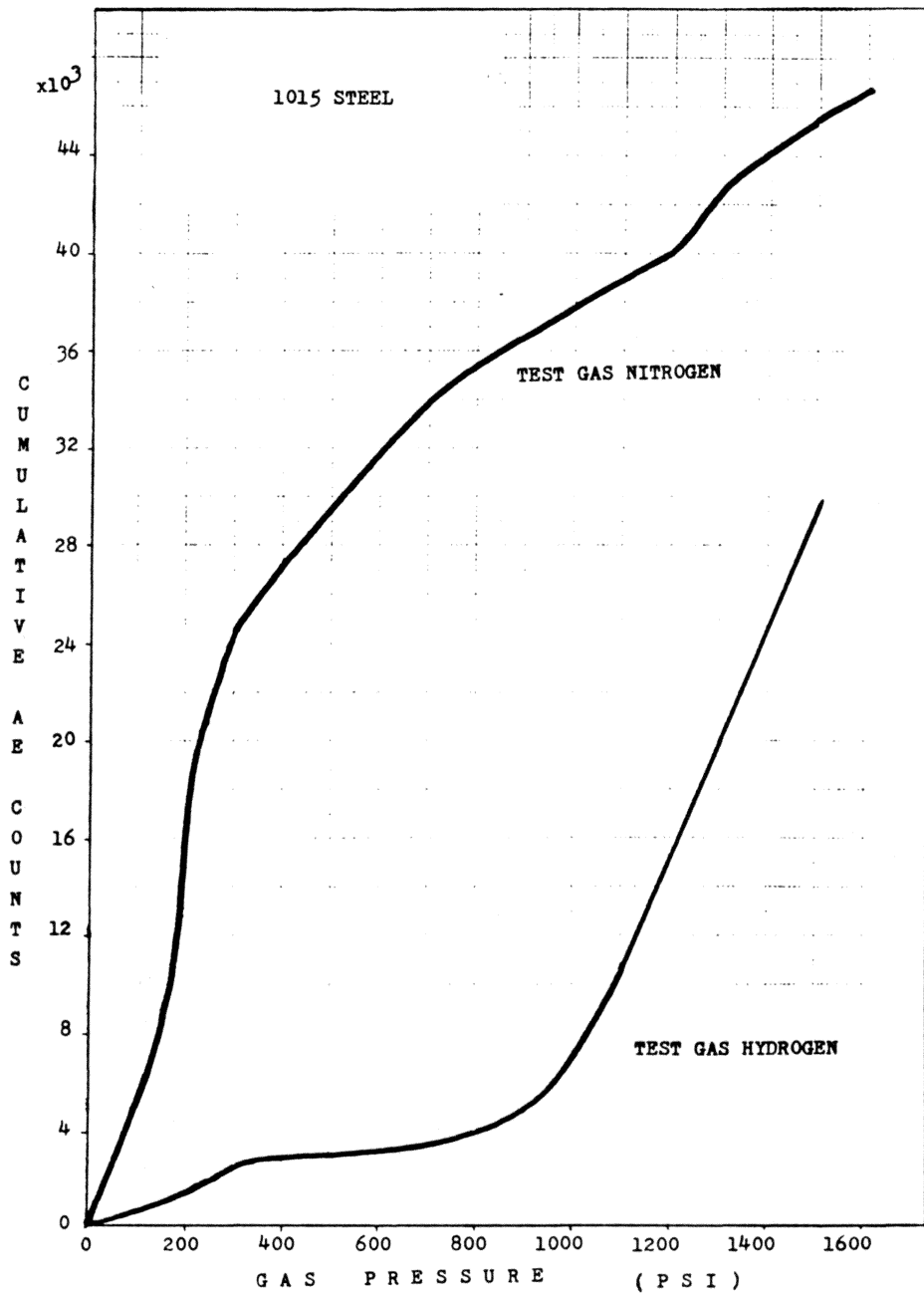


Figure 7 . Graph of cumulative acoustic emission counts vs. gas pressure for mild steel disks tested in a disk pressurization system.

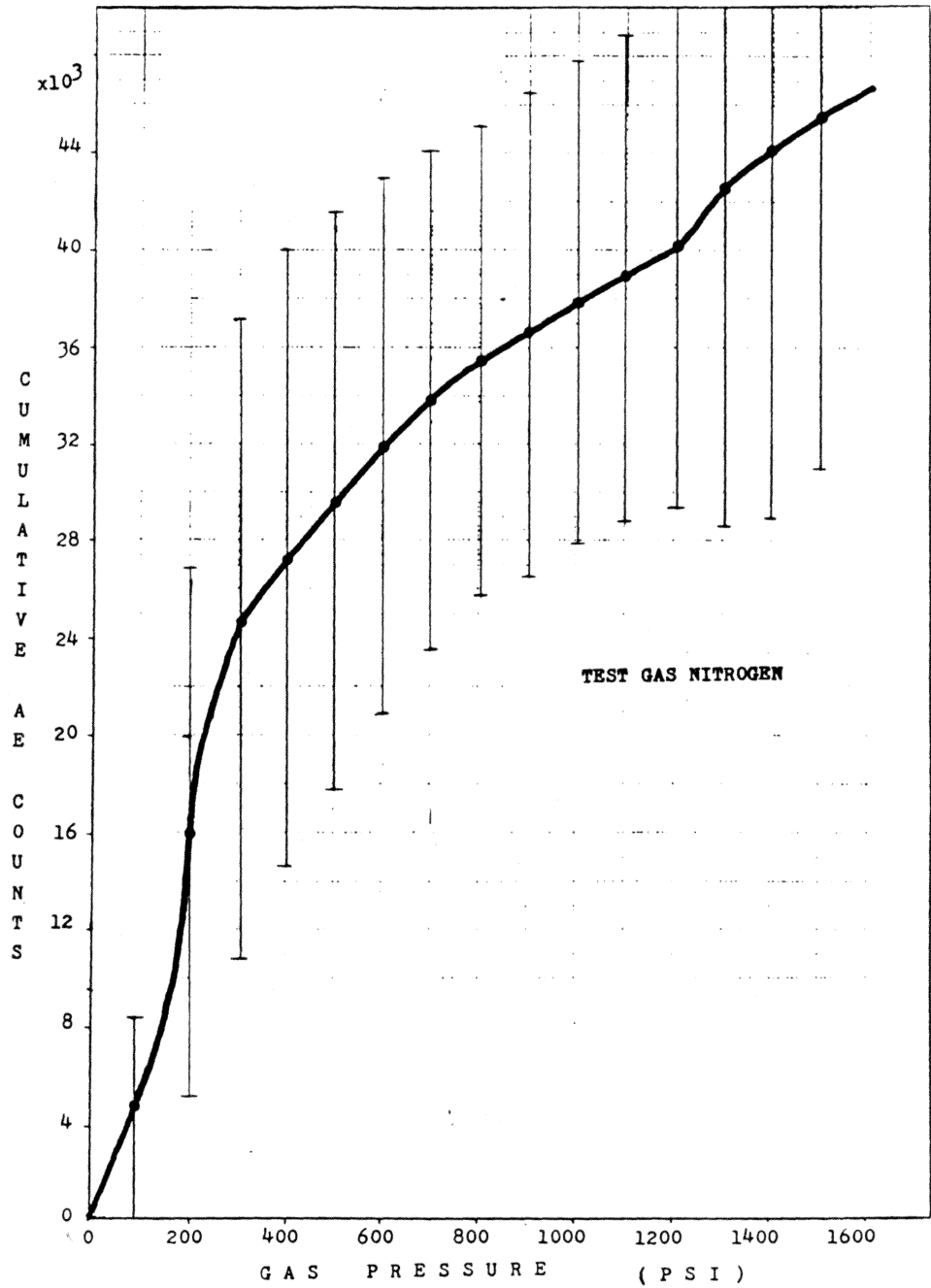


Figure 8. Cumulative AE counts vs. gas pressure of nitrogen with error bars representing plus or minus one standard deviation.

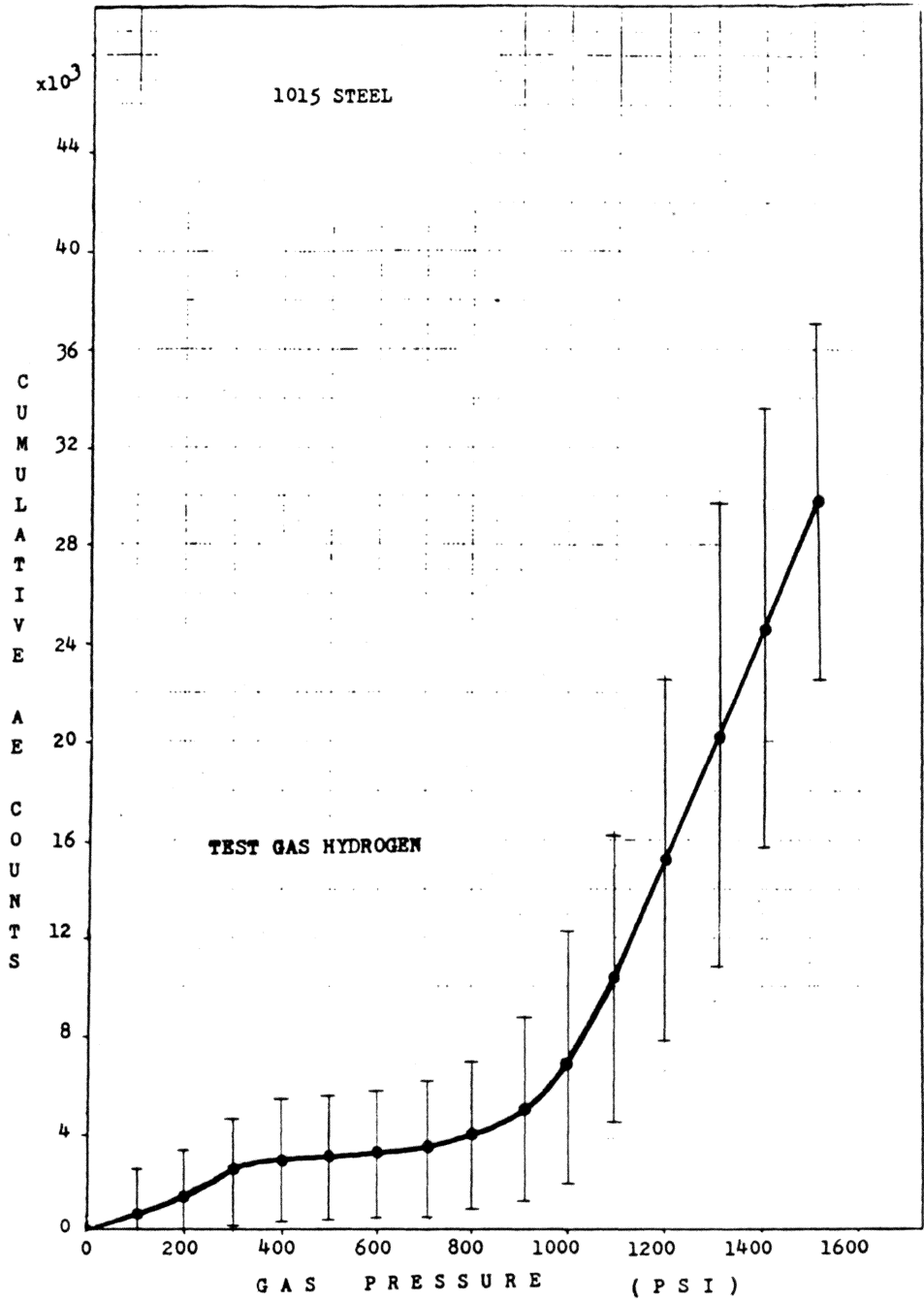


Figure 9. Cumulative AE counts vs. gas pressure of hydrogen with error bars representing plus or minus one standard deviation.

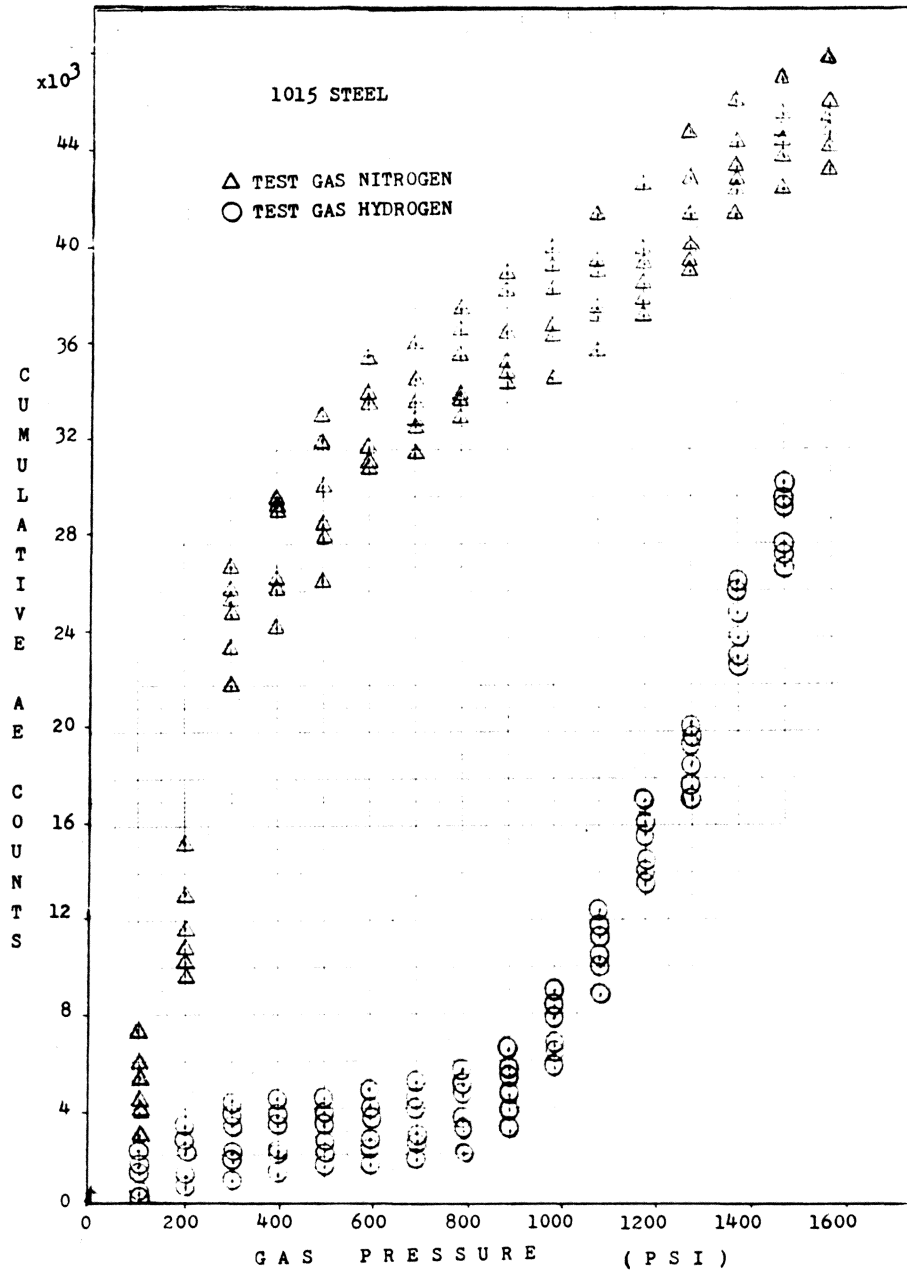


Figure 10. Plot of the actual data points used for calculating the curves in Figure 7.

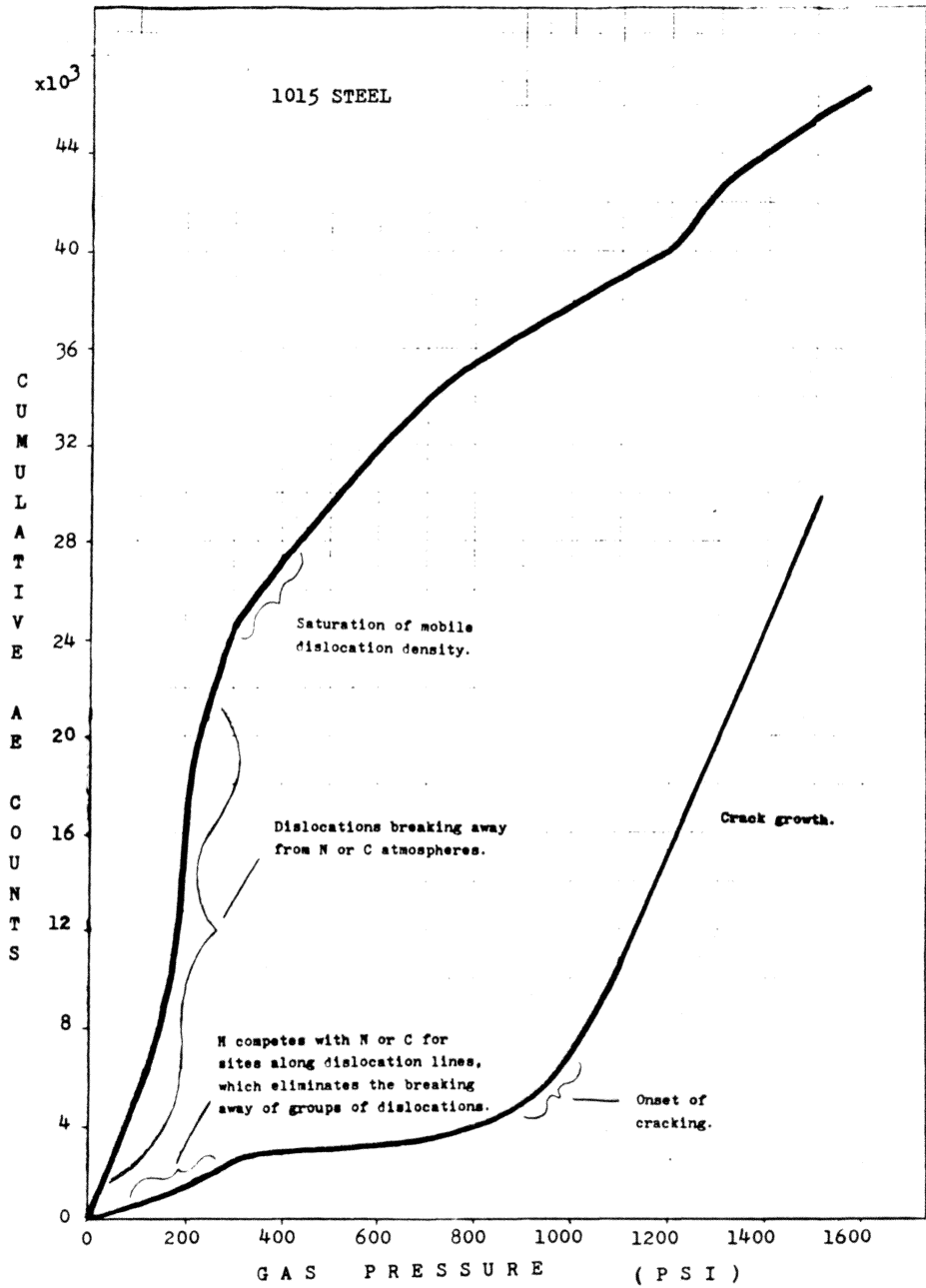


Figure II . Graph of cumulative acoustic emission counts vs. gas pressure for mild steel disks tested in a disk pressurization system. Notes indicate the occurrence of various phenomena.

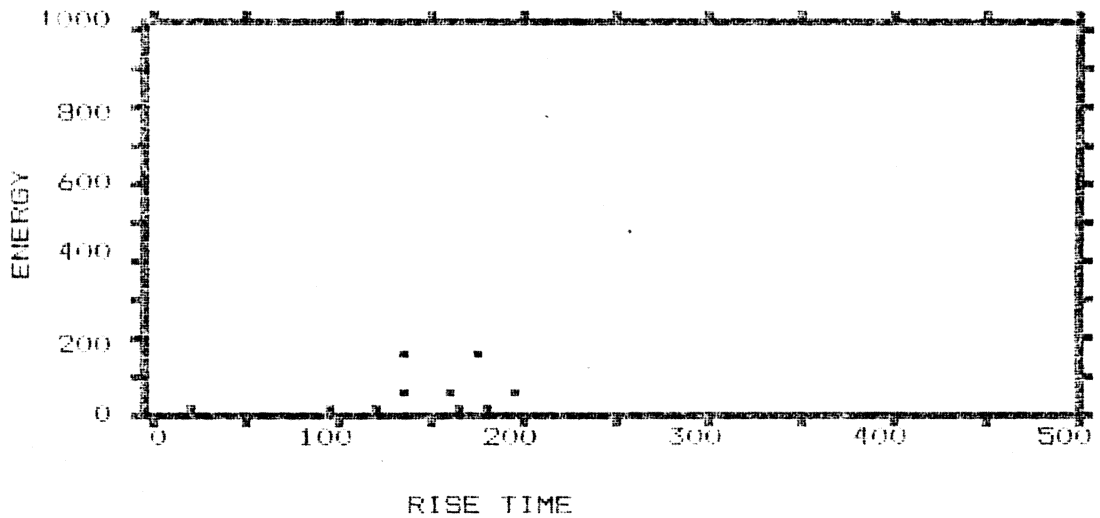
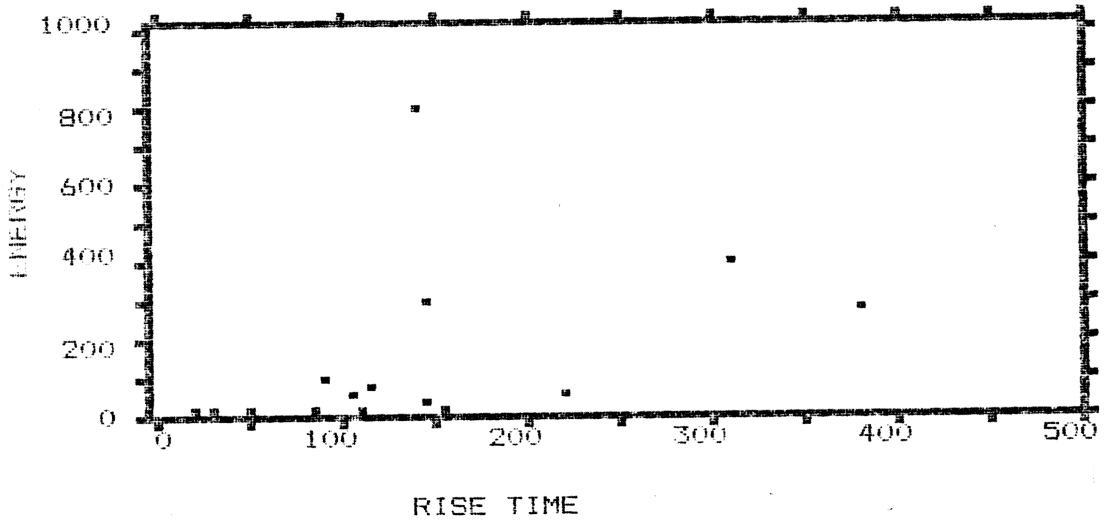


Figure 12. AE data for pressurization in nitrogen (top) and hydrogen (bottom) at a gas pressure of 200 psi. Note high energy events in the top figure.

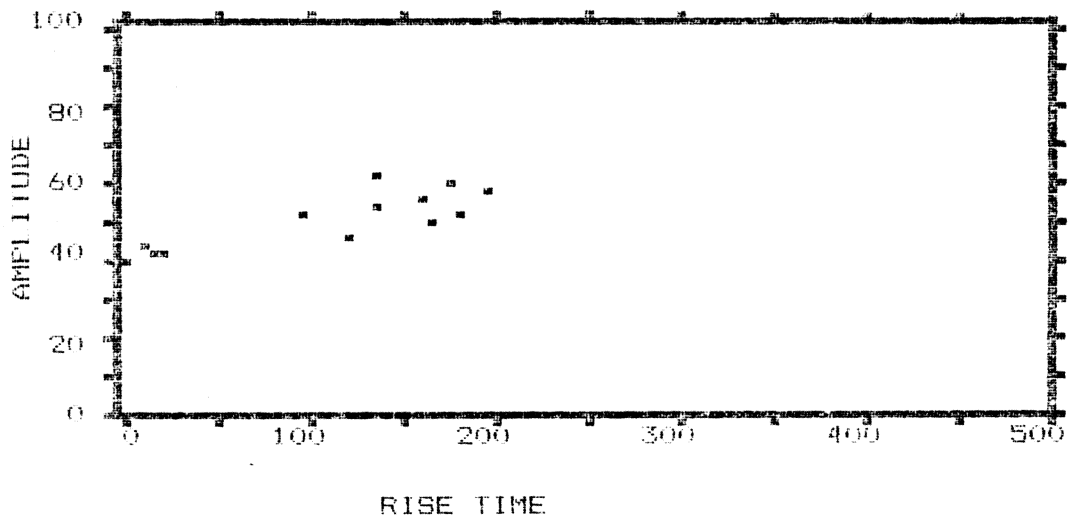
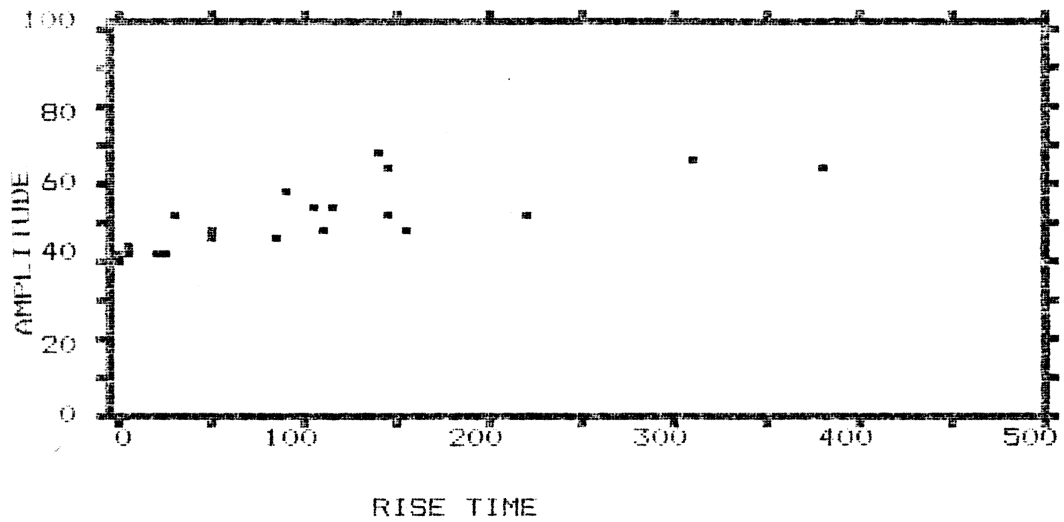


Figure 13.

AE data for pressurization in nitrogen (top) and hydrogen (bottom) at a gas pressure of 200 psi. Note high amplitude events in the top figure.

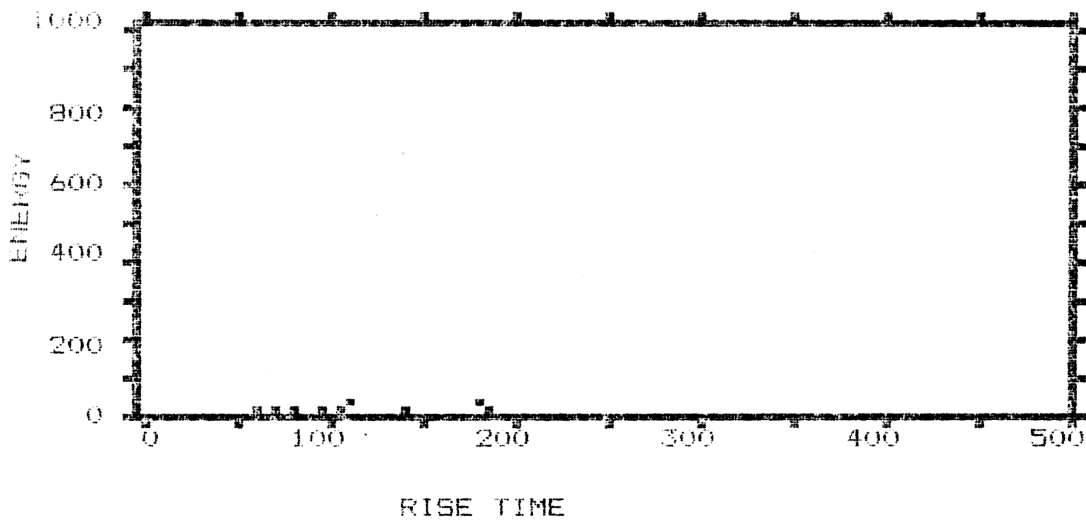
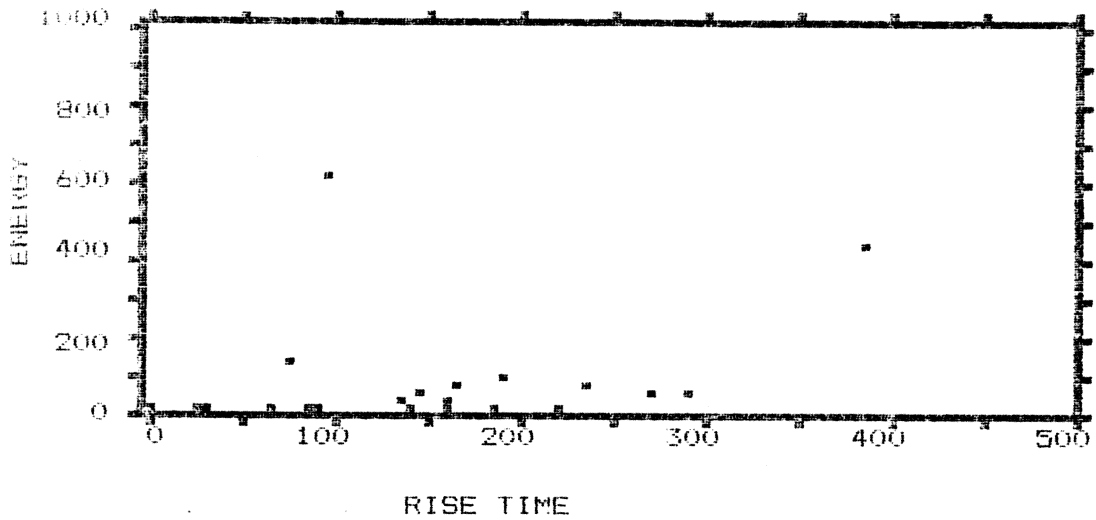


Figure 14. AE data for pressurization in nitrogen (top) and hydrogen (bottom) at a gas pressure of 250 psi. The high energy events in the top figure are believed to be from the breaking away of dislocations. These high energy events have longer rise times and lower amplitudes than high energy events from crack formation (see Figure).

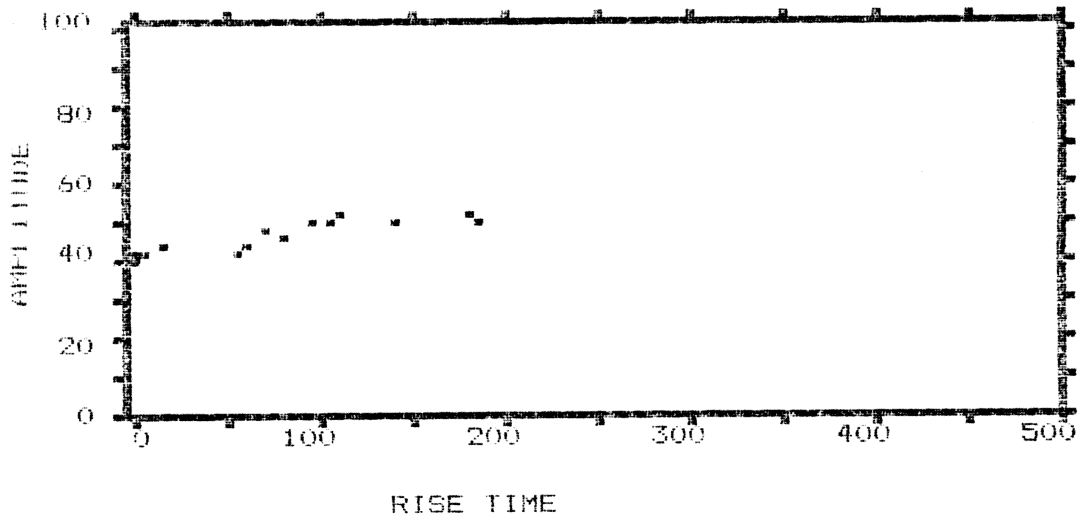
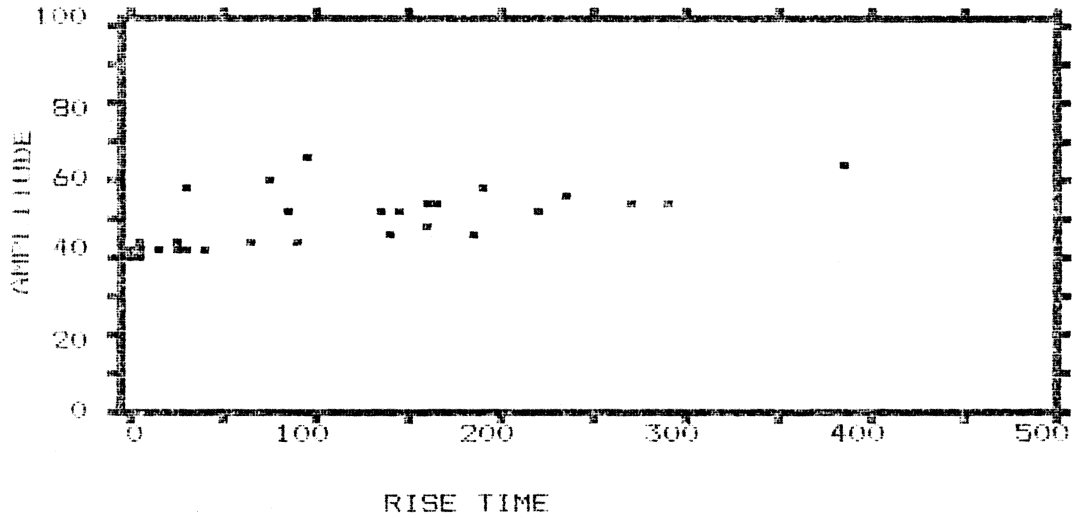


Figure 15. AE data for pressurization in nitrogen (top) and hydrogen (bottom) at a gas pressure of 250 psi. Note the numerous high amplitude events in the top figure.

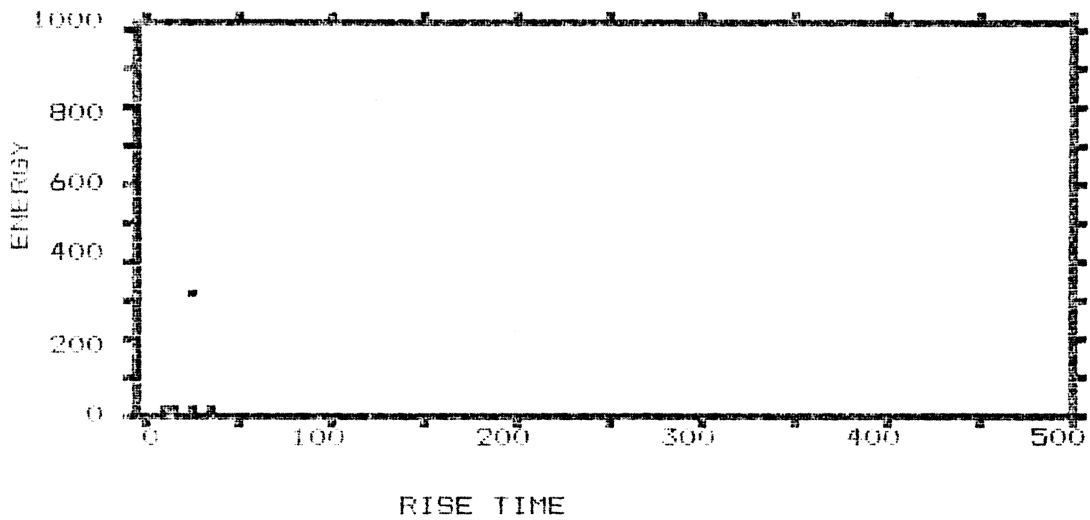
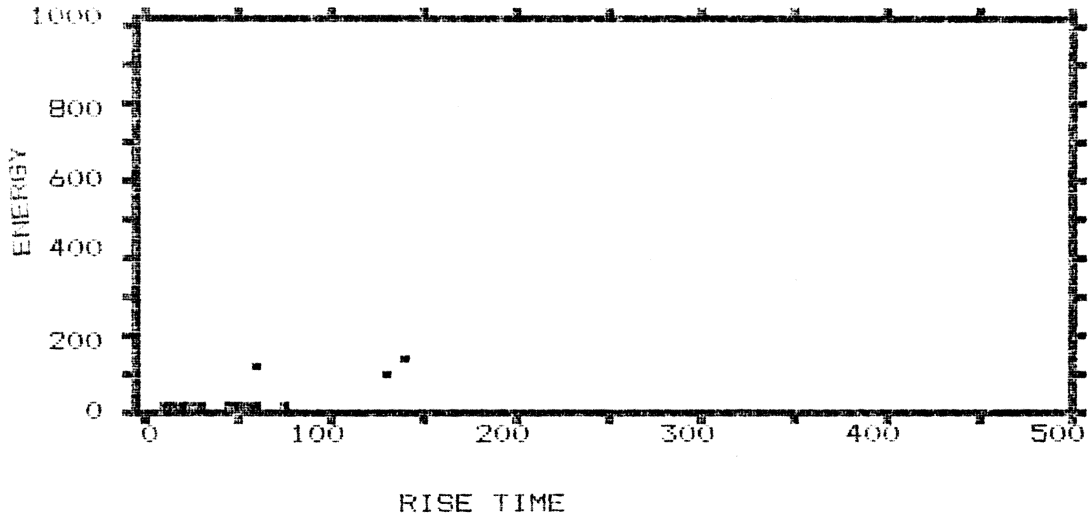


Figure 16. AE data for pressurization in nitrogen (top) and hydrogen (bottom) at a gas pressure of 950 psi. The high energy, low rise time event in the bottom figure is believed to be the signal from a crack forming.

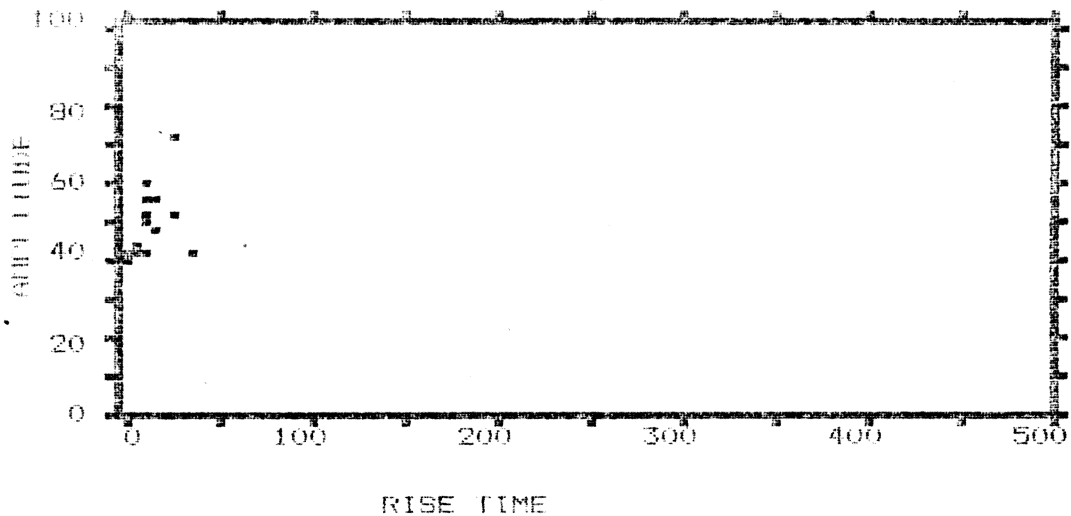
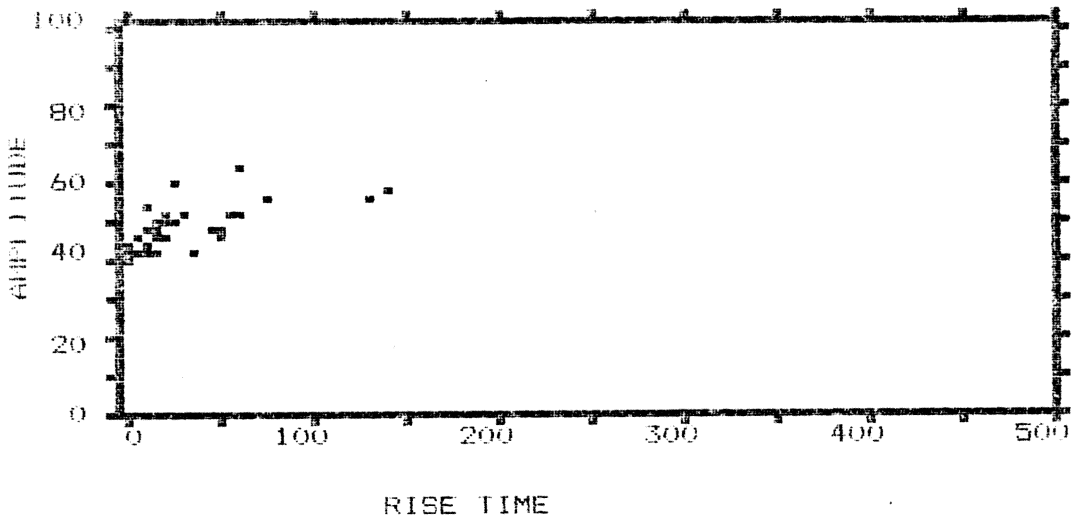


Figure 17. AE data for pressurization in nitrogen (top) and hydrogen (bottom) at a gas pressure of 950 psi. The high amplitude, low rise time event in the bottom figure is believed to be the signal from a crack forming.

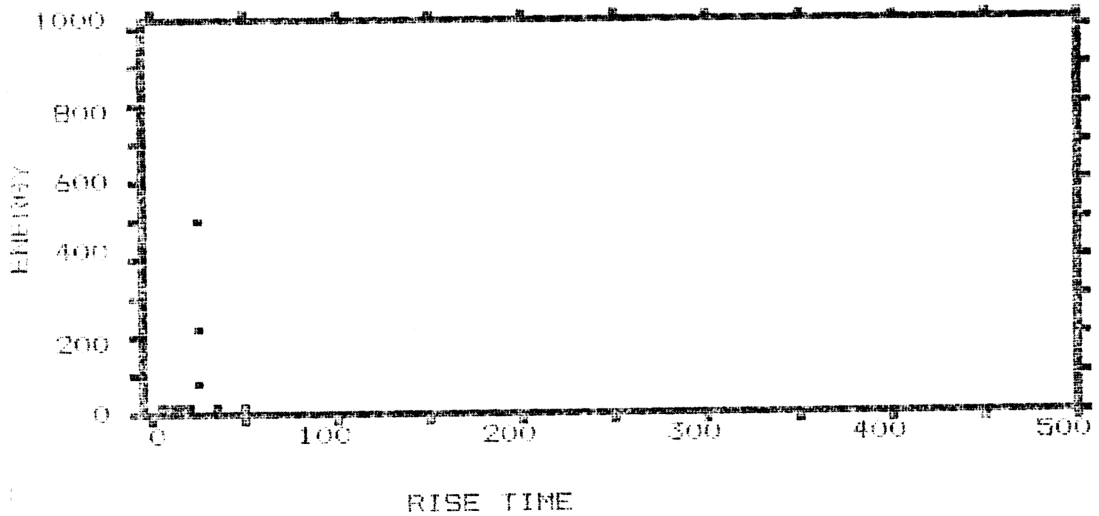
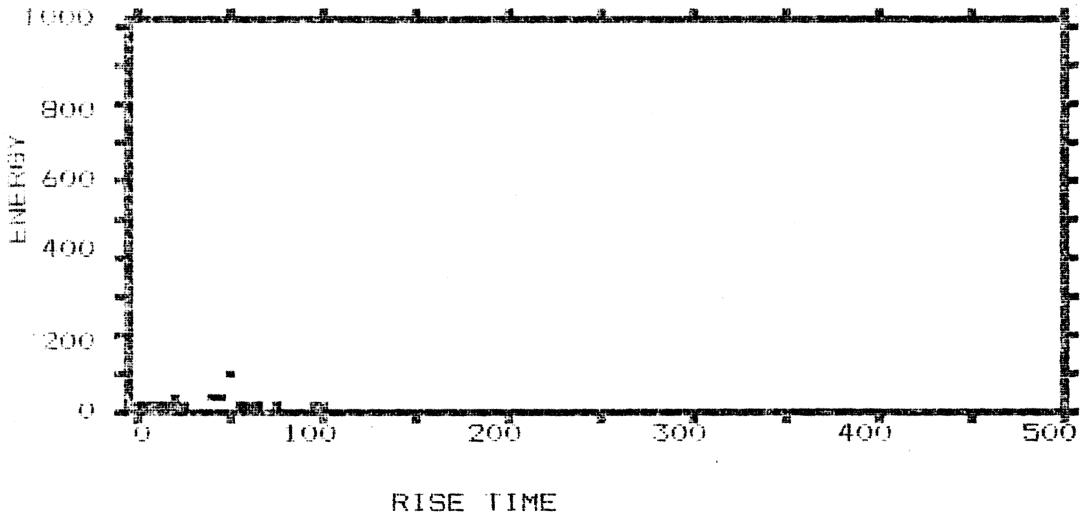


Figure 18. AE data for pressurization in nitrogen (top) and hydrogen (bottom) at a gas pressure of 1000 psi. The high energy, low rise time, high amplitude (see next figure) events in the bottom figure are the result of hydrogen enhanced cracking.

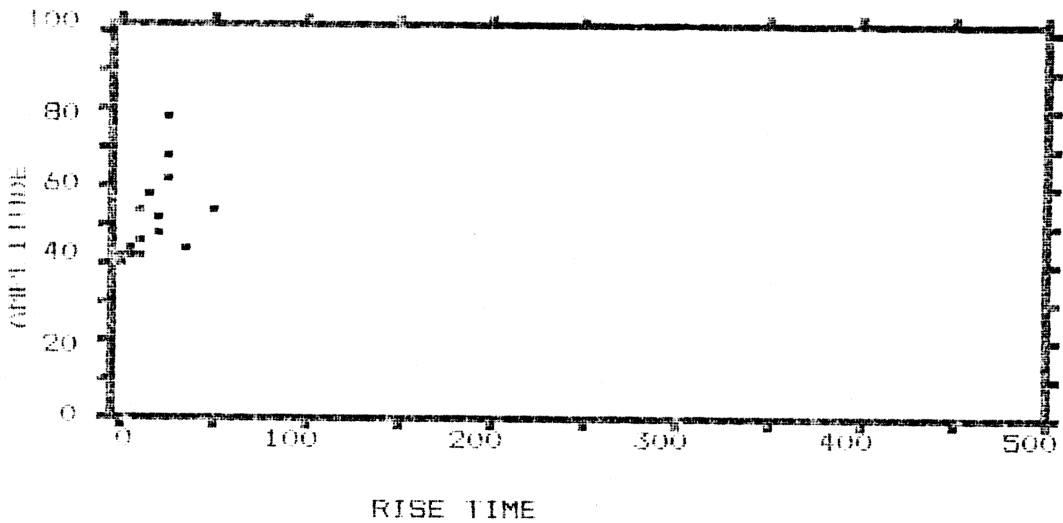
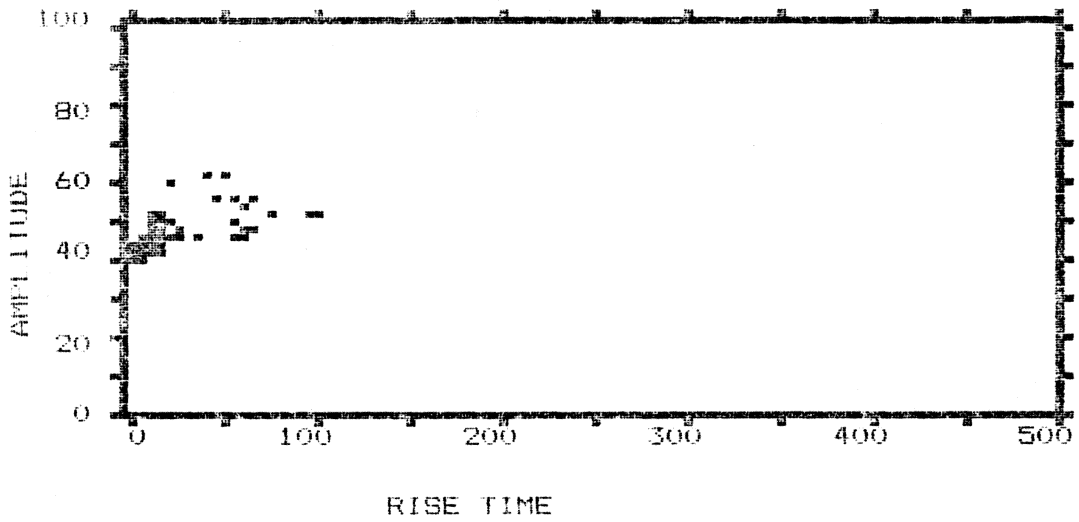


Figure 19. AE data for pressurization in nitrogen (top) and hydrogen (bottom) at a gas pressure of 1000 psi. The high energy (see previous figure), low rise time, high amplitude events are the result of hydrogen enhanced cracking.

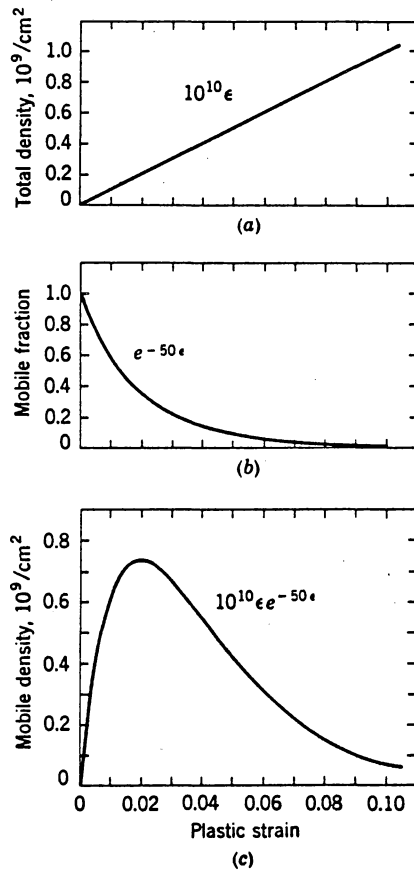


Figure 20. Schematic drawings of the changes with increasing strain of: (a) total dislocation density; (b) mobile fraction; (c) mobile dislocation density (49).

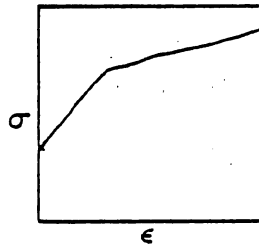
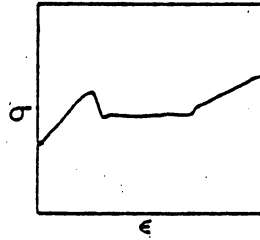


Figure 2). Schematic illustrating the difference in mechanical yielding in oxygen (top) vs. hydrogen (bottom) (50).

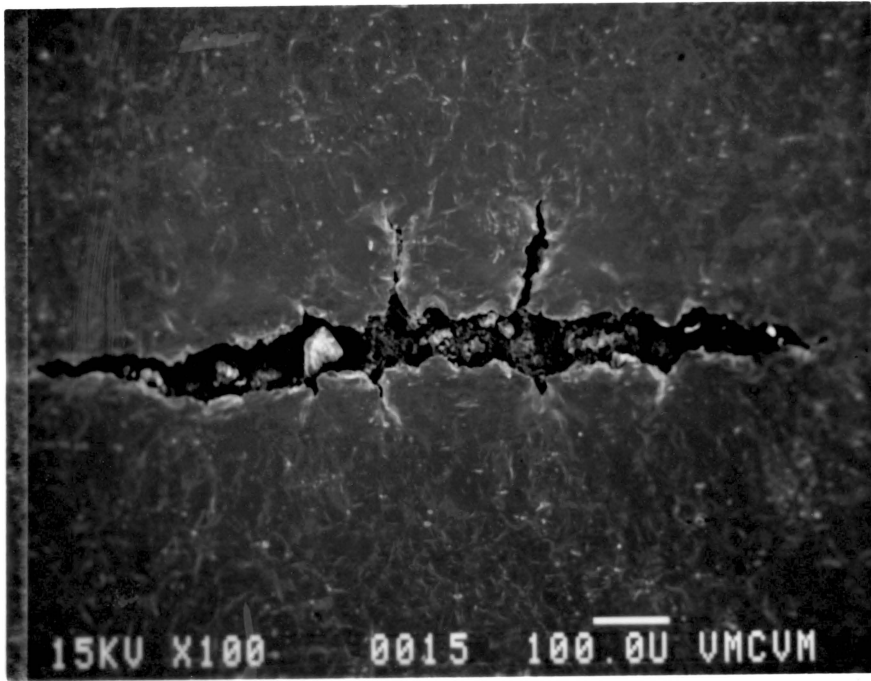


Figure 22. Crack on the surface of a disk that was pressurized in hydrogen gas to 1500 psig. The formation of the crack was detected at 1000 psig from acoustic emission signals.

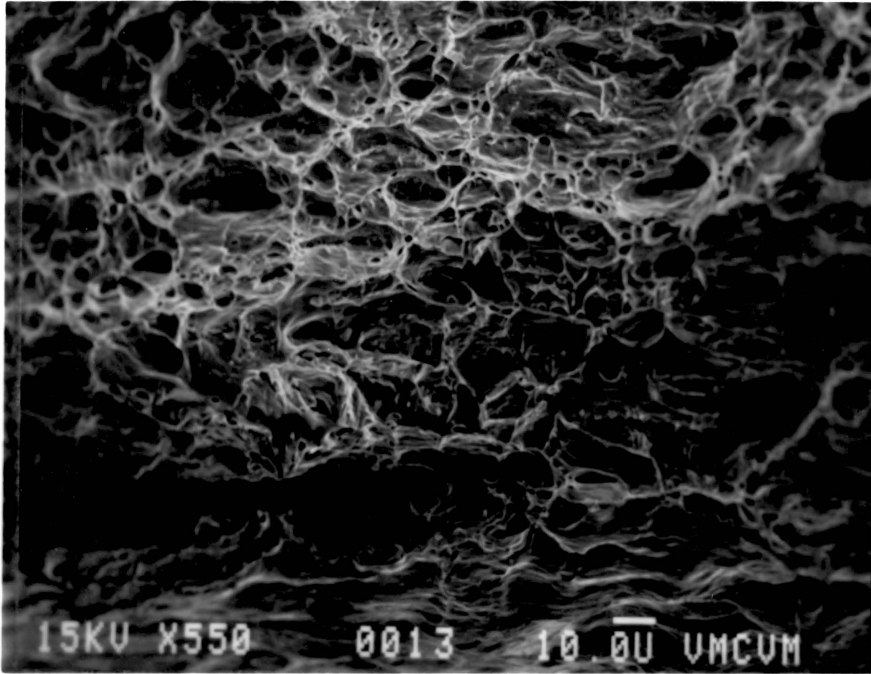


Figure 23. Fracture surface of AISI 1015 steel disk after bursting in nitrogen at a gas pressure of 1650 psi.

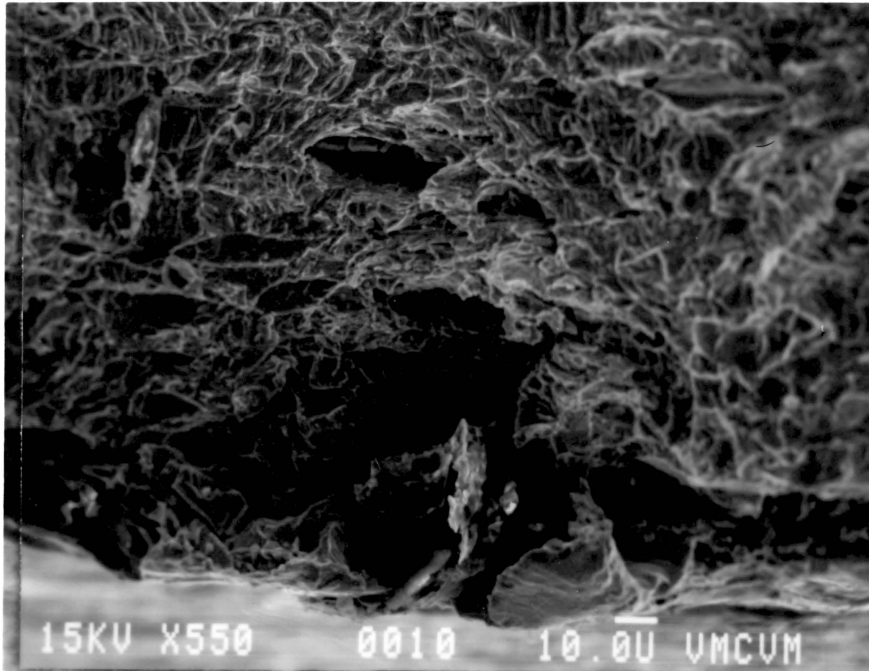


Figure 24 . Fracture surface of AISI 1015 steel disk after leaking in hydrogen at a gas pressure of 1500 psi.

Table I
ROOM TEMPERATURE MECHANICAL PROPERTIES
OF AISI 1015 STEEL

| | |
|----------------------|--------------------|
| Yield Stress | 236 MPa (34.2 ksi) |
| Ultimate Stress | 325 MPa (47.1 ksi) |
| True Fracture Stress | 594 MPa (86.2 ksi) |
| % Reduction in Area | 63% |